Neutropenia with impaired host defense against microbial infection in mice lacking androgen receptor

Kuang-Hsiang Chuang,[1] Saleh Altuwaijri,[1,2] Gonghui Li,[1,3] Jiann-Jyh Lai,[1] Chin-Yi Chu,[1] Kuo-Pao Lai,[1] Hung-Yun Lin,[1] Jong-Wei Hsu,[1] Peter Keng,[1] Ming-Chi Wu,[4] and Chawnshang Chang[1]

[1]George Whipple Laboratory for Cancer Research, Departments of Pathology, Urology, and The Cancer Center, University of Rochester Medical Center, Rochester, NY 14642
[2]Clinical Research Laboratory, Saad Specialist Hospital, Al-Khobar, Saudi Arabia 31952
[3]Department of Urology, Sir Run Run Shaw Hospital, Zhejiang University, Hangzhou, China 310016
[4]The Development Center for Biotechnology, Taipei, Taiwan 221

Neutrophils, the major phagocytes that form the first line of cell-mediated defense against microbial infection, are produced in the bone marrow and released into the circulation in response to granulocyte-colony stimulating factor (G-CSF). Here, we report that androgen receptor knockout (ARKO) mice are neutropenic and susceptible to acute bacterial infection, whereas castration only results in moderate neutrophil reduction in mice and humans. Androgen supplement can restore neutrophil counts via stabilizing AR in castrated mice, but not in ARKO and testicular feminization mutant (Tfm) mice. Our results show that deletion of the AR gene does not influence myeloid lineage commitment, but significantly reduces the proliferative activity of neutrophil precursors and retards neutrophil maturation. CXCR2-dependent migration is also decreased in ARKO neutrophils as compared with wild-type controls. G-CSF is unable to delay apoptosis in ARKO neutrophils, and ARKO mice show a poor granulopoietic response to exogenous G-CSF injection. In addition, AR can restore G-CSF–dependent granulocytic differentiation upon transduction into ARKO progenitors. We further found that AR augments G-CSF signaling by activating extracellular signal-regulated kinase 1/2 and also by sustaining Stat3 activity via diminishing the inhibitory binding of PIAS3 to Stat3. Collectively, our findings demonstrate an essential role for AR in granulopoiesis and host defense against microbial infection.

CORRESPONDENCE
Chawnshang Chang:
chang@urmc.rochester.edu

Abbreviations used: AAD, amino-actinomycin-D; AR, androgen receptor; ARKO, AR knockout; CMP, common myeloid progenitor; DHT, dihydrotestosterone; FSC, forward scatter; G-CSF, granulocyte-colony stimulating factor; GMP, granulocyte/macrophage progenitor; GST, glutathione *S*-transferase; M-CSF, macrophage-colony stimulating factor; MIP-2, macrophage-inflammatory protein-2; Q-PCR, quantitative PCR; si, small interfering; SSC, side scatter; Tfm, testicular feminization mutant.

Granulopoiesis is a dynamic process leading to the production of 120 billion granulocytes daily in humans; its synthetic capacity can be increased at least 10-fold in response to certain stress conditions, such as infection. Granulopoiesis follows an orchestrated program of cell proliferation, differentiation, and apoptosis, resulting in the expansion of a small pool of stem cells that evolve from granulocytic progenitors/precursors to mature granulocytes. Neutrophils are the most abundant type of granulocyte, whereas eosinophils and basophils are much rarer. Originating from stem cells and progenitors, neutrophils in the bone marrow are comprised of a precursor pool and a storage pool. Peripheral blood neutrophils, which are postmitotic, consist of a free circulating pool and a marginal pool.

Granulocyte-colony stimulating factor (G-CSF) plays a major role in regulating granulopoiesis (1). G-CSF not only stimulates the proliferation of granulocytic precursors (2), but also prolongs neutrophil survival (3) and reduces the mean transit time from granulocytic progenitors/precursors to mature granulocytes (4). The importance of G-CSF in granulopoiesis was demonstrated in G-CSF KO mice. These mice only have 20% of the normal circulating neutrophils and a correspondingly small neutrophil precursor pool in their bone marrow (5).

The biological action of androgens is mediated through the androgen receptor (AR), a

The Rockefeller University Press $30.00
J. Exp. Med. Vol. 206 No. 5 1181-1199
www.jem.org/cgi/doi/10.1084/jem.20082521

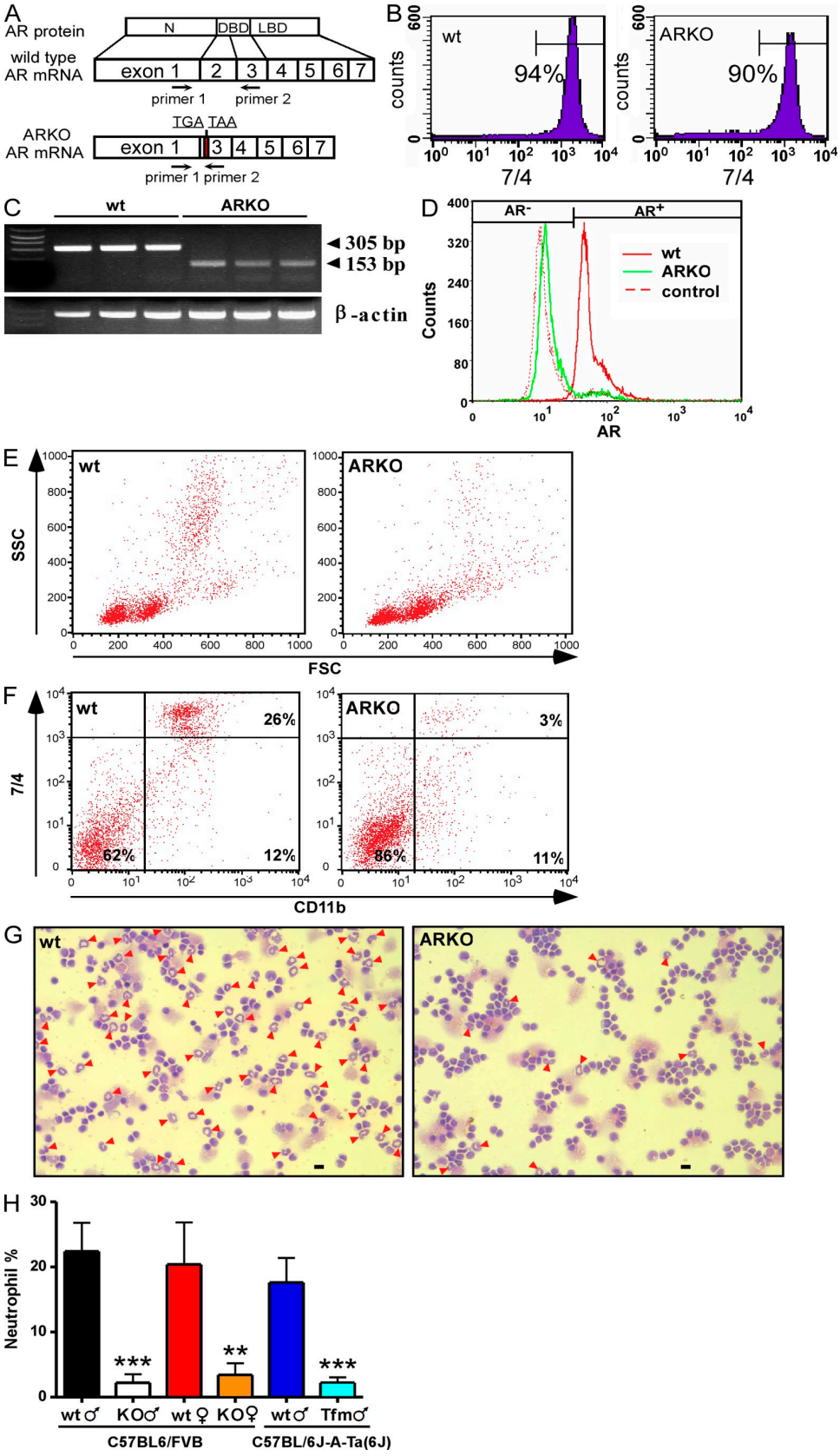

ligand-inducible nuclear receptor that regulates the expression of target genes at the transcriptional level via binding to an androgen-response element. Protein kinase A activators, such as cAMP, could activate AR transactivation activity in an androgen-independent manner (6). In addition, AR could be activated in a ligand-independent manner by epidermal growth factor, Her2/Neu, insulin-like growth factor 1, keratinocyte growth factor, and vasoactive intestinal peptide (7–9). Another study also suggested that activated G protein–coupled receptors could induce ligand-independent AR activity (10). On the other hand, it has been suggested that a nongenomic effect of AR may occur through the interaction with c-Src to induce the MAPK signal cascade (11). However, transcription-independent functions of AR remain largely unclear.

The AR gene is located on the X chromosome and plays an important role in male sexual differentiation and pubertal sexual maturation, the maintenance of spermatogenesis, and male gonadotropin regulation. Phenotype analysis shows that AR knockout (ARKO) male mice exhibited a femalelike external appearance, including a vagina with a blind end, without penis and scrotum (12). Male reproductive organs, including seminal vesicles, vas deferens, epididymis, and prostate, were lacking in ARKO male mice. Their testes are significantly smaller and serum testosterone concentrations are lower in ARKO male mice compared with WT mice. Also, spermatogenesis is arrested at pachytene spermatocytes in ARKO male mice. In female ARKO mice, retarded development of mammary glands with reduced ductal branching is shown in the prepubertal stages (13). The ovarian dysfunction and the lower mean number of pups per litter were observed in adult ARKO female mice (14, 15). In addition to reproductive defects, the number/size of adipocytes and the body weight were also found to be decreased in ARKO mice (12).

It has been reported that AR broadly expresses in neutrophil-lineage cells from the myeloblast stage to the mature neutrophil stage with no difference in the pattern of AR expression between male and female (16). Androgen was found to stimulate proliferation of committed erythrocytic and granulocytic precursors in vitro (17–20), and accelerate recovery of leukocytes after radiation or chemotherapy (21–25). Clinical observations with androgens in the treatment of aplastic anemia (26, 27), Fanconi's anemia (28, 29), and during therapy with myelosuppressive agents (30, 31) suggest that androgen might increase neutrophil production. A clinical study with polycystic ovary syndrome patients who have high serum androgen levels showed higher neutrophil counts (32), also suggesting that androgen/AR might be associated with granulopoiesis. However, it is still unclear how androgen and AR regulate neutrophil homeostasis.

RESULTS

Targeted disruption of the AR gene in ARKO mice

Because male infertility is observed in testicular feminization mutant (Tfm) mice, which carry an unstable truncated AR mutant (33), it is impossible to generate female homologous AR deletion mice by conventional gene disruption methods. To solve this difficulty, we used the Cre–loxP technique to generate a mouse model with the targeted disruption of AR (ARKO) (12). We successfully generated ARKO mice of both genders and WT littermates, and further used these mice to investigate if loss of AR influences neutrophil production. In ARKO mice, the deletion of exon 2 in AR (Fig. 1 A) results in a splice between exon 1 and exon 3, creating two sequential nonsense mutations at new amino acid positions 533 and 534, leading to premature termination of the AR protein. RT-PCR analyses of total RNA extracted from isolated bone marrow neutrophils (Fig. 1 B) showed that the mRNA from ARKO neutrophils lacked the 305-bp fragment from exon 2 of AR (Fig. 1 C), evidence that the intact AR is not expressed in ARKO neutrophils and precursors. Intracellular analysis of endogenous AR protein by flow cytometry further confirmed that AR protein expression occurs in WT, but not ARKO, bone marrow neutrophils (Fig. 1 D).

ARKO mice have low numbers of neutrophils in circulation

We then examined circulating neutrophils in ARKO and WT mice by FACS analyses. On the basis of forward scatter (FSC) and side scatter (SSC), FACS analyses of peripheral blood leukocytes showed that a high-SSC population (i.e., a granulocyte population) was barely detectable in ARKO mice (Fig. 1 E). Using FACS analysis with neutrophil-specific monoclonal antibodies (clone 7/4) and anti-CD11b antibodies, we found that only 3% of leukocytes were neutrophils in ARKO mice, in contrast to 26% neutrophils in WT mice (Fig. 1 F). Neutrophils were rarely found in cytospin smears of blood leukocytes from ARKO mice (Fig. 1 G). As shown

Figure 1. AR-targeted disruption and analysis of peripheral neutrophils in ARKO mice. (A) Schematic representation of murine AR protein domains and corresponding exons in AR mRNA. The AR mRNA is composed of seven exons; exon 2 is removed in ARKO mice. DBD, DNA-binding domain. LBD, ligand-binding domain. (B) The purity of isolated bone marrow neutrophils from WT and ARKO mice is >90%. (C) Using the primers 5′-AATGGGACCTTGGATGGAGAAC-3′ and 5′-TCCCTGCTTCATAACATTTCCG-3′, an AR transcript of 305 bp will be obtained from WT AR, but only 153 bp when floxed exon 2 is deleted. Full-length AR mRNA is not expressed in neutrophils isolated from bone marrow of AR-deficient mice. (D) Intracellular AR protein is not detected in neutrophils isolated from bone marrow of AR-deficient mice. Nonspecific IgG was used as primary antibody for the control. (E) FACS analysis of peripheral blood from 8-wk-old WT and ARKO mice. FSC and SSC of peripheral leukocytes show significant decreases of high-SSC granulocytic population in ARKO mice ($n = 4$) compared with WT littermates ($n = 4$). (F) FACS analyses with neutrophil-specific antibodies (clone 7/4) and anti-CD11b antibodies. Neutrophils are drastically reduced in ARKO mice ($n = 4$) compared with WT littermates ($n = 4$). (G) Representative photomicrographs of Wright-Giemsa–stained cells on cytospins from blood after erythrocyte lysis. Neutrophils (arrow heads) are rarely found on leukocyte cytospins from ARKO mice compared with WT controls. Bar, 10 µm. (H) Manual differential counting of neutrophils was performed on blood smears from 9-wk-old sex-matched (WT), ARKO (KO), and Tfm male mice. Results are representative of four separate experiments ($n = 4$ per group). Data represent the mean ± SD. **, $P < 0.01$ compared with WT mice. ***, $P < 0.001$ compared with WT mice.

by examination of blood smears with Wright-Giemsa staining, male and female ARKO mice have normal white blood cell counts, but very low percentages of neutrophils in peripheral blood (Fig. 1 H). Examining blood smears from Tfm mice (Fig. 1 H), we confirmed that loss of AR results in a significantly reduced neutrophil abundance in peripheral leukocytes. Automated blood analysis revealed that the numbers of total white blood cells, red blood cells, and platelets remained comparable in ARKO mice (Table I A). The mean differential ratio of peripheral lymphocytes in ARKO mice was increased from 75 to 94% without obvious alterations in monocyte and eosinophil numbers (Table I B). However, there was a significant reduction of neutrophils in blood compared with WT mice (Table I B). These results suggest that the AR might play a critical role in sustaining a normal number of circulating neutrophils in vivo.

Neutrophils are reduced in bone marrow of ARKO mice

We then sought to determine if the neutropenia in ARKO mice was caused by a defect in granulopoiesis in the bone marrow. We found that the high SSC granulocyte population in bone marrow was markedly decreased in ARKO mice (Fig. 2 A). Further analysis of the granulocyte population with clone 7/4 and CD11b antibodies demonstrated a 50% decrease of neutrophils in bone marrow of ARKO mice compared with those in WT littermates (Fig. 2 B). These results demonstrated that loss of AR results in significant reduction of neutrophils in bone marrow.

To learn if both androgen and AR are required for neutrophil production, we examined the effects of castration and androgen supplementation on neutrophil counts in WT, ARKO, and Tfm mice. We found that castration of normal mice only results in a relatively moderate reduction of neutrophils as compared with neutropenia in ARKO and Tfm mice (Fig. 2, C–E), and supplement of exogenous dihydrotestosterone (DHT) restores neutrophils in castrated mice, but not in ARKO and Tfm mice (Fig. 2, C–E). These results suggest that AR, but not androgen, is required for neutrophil homeostasis.

Androgen ablation reduces neutrophil counts, but does not result in neutropenia in humans

We also compiled blood cell counts from 33 advanced prostate cancer patients before and after the surgical castration therapy. Those patients had no prior history of chemotherapy and radiation therapy, and had no sign of infection (WBC counts were <10,000 per μl). The results showed that their neutrophil differential counts only moderately decreased after surgical castration therapy (Fig. 2 F). The decrease of neutrophil counts in those patients with surgical castration was not as significant as that observed in ARKO mice, further supporting that androgen is less important than AR in neutrophil homeostasis.

Table I. Blood and bone marrow analysis

Blood/bone marrow	WT	ARKO	Statistics
A. Blood parameters	WT (n = 24)	ARKO (n = 18)	P-value
WBC ($\times10^3/\mu l$)	1.83 ± 0.77	1.93 ± 0.78	0.690
RBC ($\times10^6/\mu l$)	9.18 ± 0.97	9.31 ± 0.6	0.603
Platelets ($\times10^3/\mu l$)	643 ± 192	573.8 ± 156	0.203
Hemoglobin (g/dl)	13.69 ± 1.04	13.43 ± 0.86	0.391
Hematocrit (%)	49.88 ± 4.66	47.06 ± 2.88	0.021
MCV (fl)	54.5 ± 2.73	50.61 ± 3.15	<0.001
MCH (pg)	15.17 ± 1.05	14.39 ± 0.7	0.006
MCHC (g/dl)	27.54 ± 1.64	28.61 ± 1.58	0.039
Lymphocytes (per μl)	1359 ± 565	1815 ± 717	0.033
Neutrophils (per μl)	420 ± 247	76 ± 59	< 0.001
B. Differential WBC	WT (n=24)	ARKO (n = 18)	P-value
Lymphocytes (%)	74.6 ± 7.7	94.7 ± 3.2	<0.001
Neutrophils (%)	22.6 ± 7.2	3.7 ± 2.2	<0.001
Eosinophils (%)	0.7 ± 0.6	0.6 ± 0.5	0.776
Monocytes (%)	2 ± 1.7	1.2 ± 0.8	0.730
C. Bone marrow analysis	WT (n=6)	ARKO (n = 6)	P-value
Myeloblasts (%)	0.6 ± 0.3	0.5 ± 0.3	0.381
Promyelocytes (%)	2.3 ± 0.6	2.2 ± 0.4	0.583
Myelocytes and metamyelocytes (%)	15 ± 1.6	10.3 ± 1.4	<0.001
Neutrophils (include Band form) (%)	32 ± 2.5	12 ± 1.8	<0.001
Bone Marrow Nucleated Cells ($\times10^6$)	33.3 ± 1.24	34.1 ± 0.8	0.244

All mice for blood and bone marrow analysis range from 8 to 12 wks old. Blood parameters from blood samples obtained from heart punctures were measured using an Abbot CELL-DYN 4000 system. 100-count leukocyte differentials were examined on blood smears from 18–24 mice in each genotype. Bone marrow analysis was based on 1,000-count manual leukocyte differentials performed on bone marrow–nucleated cells recovered from femurs of age-matched mice from each genotype. Mean values ± SD obtained from the indicated number of mice (n) are given. WBC, white blood cell count; RBC, red blood cell count; MCV, mean cell volume; MCH, mean corpuscular hemoglobin; MCHC, mean corpuscular hemoglobin concentration.

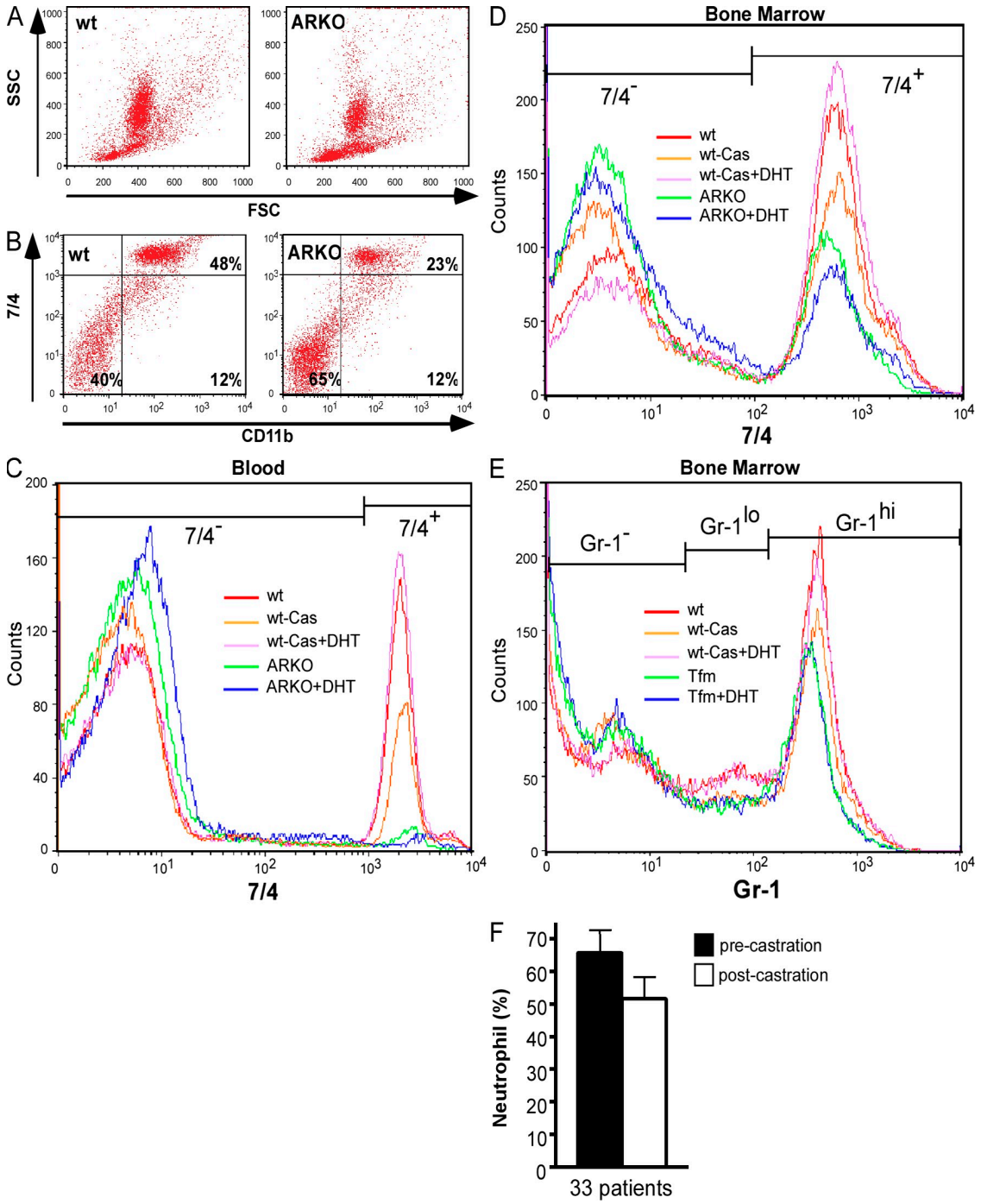

Figure 2. Analysis of bone marrow neutrophils in ARKO mice. (A) FSC/SSC analysis of bone marrow cells shows reduction of a cell population with granulocyte characteristics in 8-wk-old ARKO mice ($n = 4$) compared with WT littermates ($n = 4$). (B) Gated with CD45$^+$, FACS analyses show that bone marrow neutrophils are significantly decreased in AR-deficient mice ($n = 4$) compared with WT littermates ($n = 4$). (C) FACS analysis with antibodies against neutrophils in peripheral blood from 10-wk-old sham-operated WT, castrated (WT-Cas), castrated mice implanted with DHT-releasing pellet (WT-Cas+DHT), sham-operated ARKO (ARKO), and sham-operated ARKO mice implanted with DHT-releasing pellet (ARKO+DHT). For each group, 10^5 cells from each of four mice were pooled and analyzed. Data were analyzed using CellQuest software; neutrophil populations are shown as histograms. DHT supplementation restores neutrophil numbers in peripheral blood of castrated mice, but not in ARKO mice. (D) DHT supplementation restores bone marrow neutrophils (neutrophil-specific antibody, clone 7/4, labeled) in castrated mice, but not in ARKO mice. (E) DHT supplementation also restores neutrophils (Gr-1 labeled) in bone marrow of castrated mice, but not in those of Tfm mice. (F) Neutrophil differential counts are only moderately reduced in patients after androgen ablation therapy. Blood analysis data were collected from 33 advanced prostate cancer patients before and after surgical castration. Neutrophil differential counts are shown and presented as the mean ± SD. Animal experiments were independently performed at least three times, and representative results from one experiment are shown.

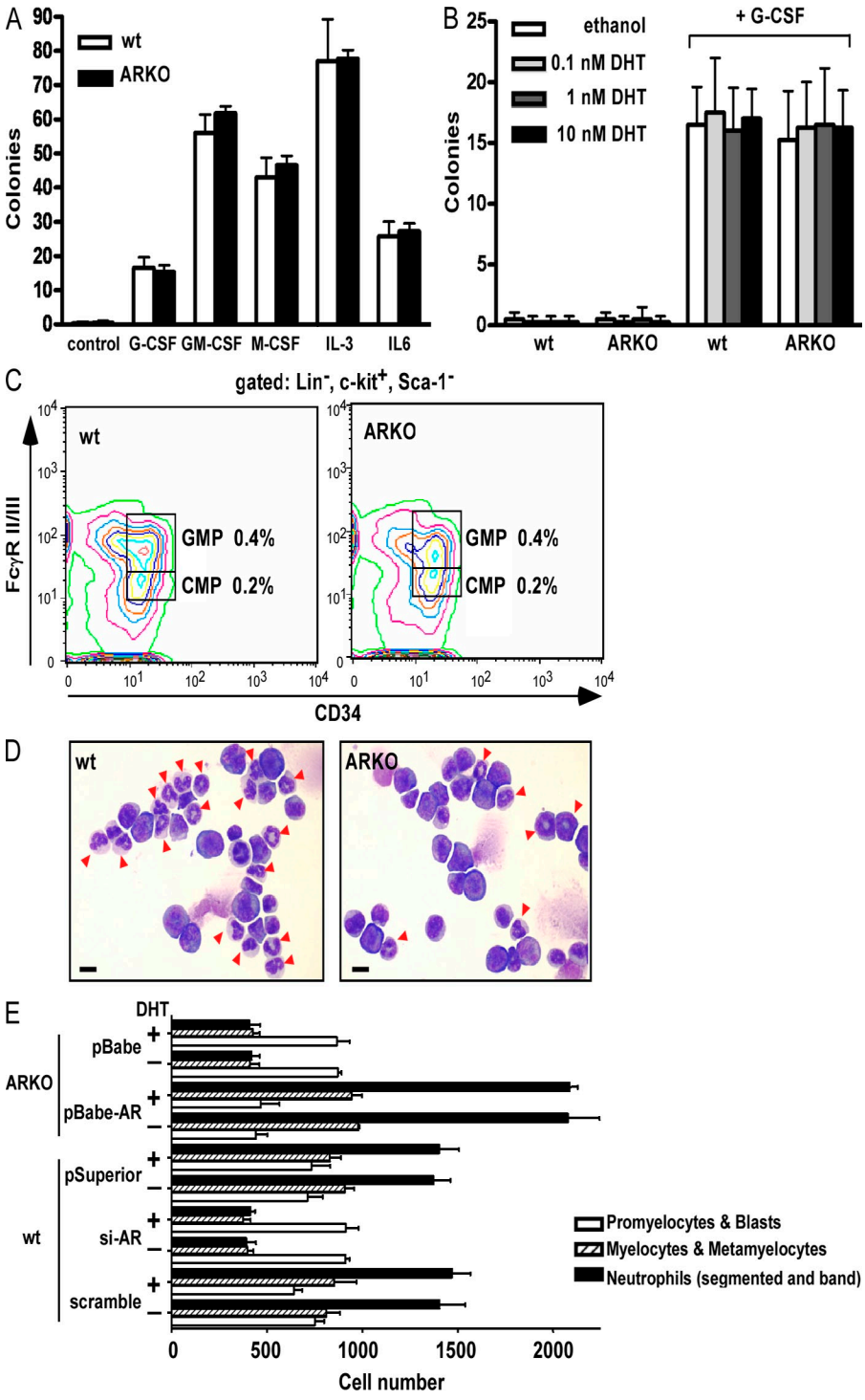

Figure 3. AR knockdown in WT myeloid progenitors by RNA interference (RNAi) suppresses neutrophil differentiation, and restoring AR in ARKO cells induces neutrophil differentiation. (A) Bone marrow cells were plated in methylcellulose-containing media supplemented with the indicated cytokine and hematopoietic colonies containing >30 cells were scored after 7 d. We analyzed bone marrow cells from five 9-wk-old animals of each genotype. (B) Effect of adding various concentrations of DHT on colony formation of mouse bone marrow cells in methylcellulose-containing media supplemented with G-CSF. (C) The populations of GMPs and CMPs are comparable in bone marrow between WT and ARKO mice. GMPs were further isolated from WT and ARKO bone marrow using FACS sorting. (D) Representative photomicrographs of isolated neutrophils and precursors from bone marrow stained with Wright-Giemsa. A decrease of nuclei-segmented neutrophils (arrow heads) in ARKO bone marrow is observed when compared with the control. Bar, 10 µm. (E) GMPs were infected with retroviruses carrying pBabe vector, pBabe-AR, pSuperior vector, pSuperior-siAR, and pSuperior-scramble. Transduced GMPs were cultured in the presence of G-CSF (10 ng/ml) with or without 10 nM DHT for 7 d. Green fluorescent colony cells were then collected and

ARKO mice have a defect in granulopoiesis between proliferative precursors and mature neutrophils with normal numbers of myeloid progenitors

We next asked which stages during granulopoiesis in bone marrow are responsible for neutropenia in ARKO mice. Using colony-forming assays, we discovered that adding G-CSF, GM-CSF, macrophage-colony stimulating factor (M-CSF), IL-3, and IL-6 induced similar levels of colony formation in ARKO bone marrow cells and WT cells in low-androgen methylcellulose medium (Fig. 3 A). Adding DHT did not influence colony numbers induced by G-CSF (Fig. 3 B). These results suggest that the populations of early granulocytic and monocytic progenitor cells are comparable in WT and ARKO bone marrow cells. Thus, we conclude that neutrophil lineage commitments in ARKO mice must be similar to those in WT mice. In addition, using FACS analyses, we found that the abundance of both common myeloid progenitors (CMPs) and granulocyte/macrophage progenitors (GMPs) in bone marrow is also comparable between WT and ARKO mice (Fig. 3 C). Using Wright-Giemsa staining of bone marrow smears, we found that fewer isolated bone marrow neutrophils from ARKO mice than from WT mice had segmented nuclei (Fig. 3 D). Differential counting of bone marrow cells showed that ARKO mice had a decrease in myelocytes/metamyelocytes and a marked decrease in mature neutrophils as compared with bone marrow cells from WT mice (Table I C). Although we observed that cancellous bone volumes of ARKO male mice are reduced compared with WT littermates (12), there is no difference in bone marrow cellularity (Table I C). These results suggest that the defect in granulopoiesis of ARKO mice occurs during the transition between proliferation of precursors (myeloblasts, promyelocytes, and myelocytes) and maturation of neutrophils (metamyelocytes, band forms, and neutrophils), leading to a defect in terminal differentiation of neutrophils.

Restoration and knockdown of AR in GMPs influence neutrophil differentiation

To see if restoration of AR rescues neutrophil differentiation, we infected FACS-sorted ARKO GMPs with retroviruses carrying the cDNA for AR and GFP or retroviruses carrying GFP alone, and then seeded infected cells into methylcellulose medium in the presence of G-CSF. Fluorescent colonies were harvested after 7 d. ARKO colonies infected with retroviruses carrying GFP alone exhibited fewer mature neutrophils (Fig. 3 E). In contrast, colonies from ARKO GMPs infected with retroviruses expressing functional AR consisted of more mature neutrophils, suggesting that the defects in neutrophil maturation resulting from ablation of AR can be rescued by AR overexpression. Again, we found that adding androgen did not result in an additional rescue on neutrophil maturation (Fig. 3 E). Also, we infected WT GMPs with retroviruses carrying AR-small interfering (si)RNA to see if knockdown of endogenous AR retards neutrophil differentiation. We confirmed the AR-siRNA knockdown efficiency with reporter assays (Fig. S1) and immunoblot analyses of AR protein expression in cells infected with retroviruses carrying AR-siRNA and scramble siRNA control (Fig. S2). Colonies from sorted WT GMPs infected with retroviruses carrying AR-siRNA and GFP showed fewer mature neutrophils than those infected with retroviruses carrying scrambled siRNA and GFP or GFP alone (Fig. 3 E). These results are consistent with the ARKO mouse data, suggesting that knockdown of endogenous AR by siRNA in GMPs could retard neutrophil maturation. Results from these complementary methods of AR manipulation in cultured cells are consistent with our in vivo ARKO mice data showing that loss of AR results in retardation of neutrophil differentiation.

Reduced proliferative activity in neutrophil precursors in bone marrow of ARKO mice

We next examined granulocytic proliferation via analysis of the cell cycling status of granulocytes within bone marrow, by labeling cells with anti–Gr-1 antibodies and propidium iodide. The proportion of cells in S and G2/M phase was lower in Gr-1$^+$ bone marrow cells from ARKO mice (Fig. 4 A), suggesting that the rate of granulocytic proliferation in bone marrow from ARKO mice is lower than in WT mice.

To learn more about the dynamics of neutrophil production in WT and ARKO mice, we labeled mitotic progenitors/precursors in vivo by intraperitoneal injection of BrdU, which only labels proliferating cells. Cells derived from the neutrophil precursor pool can be labeled with BrdU because these cells are proliferating and have matured into granulocytes, which are then released from the bone marrow into the circulation. At 96 h after the injection, the BrdU-labeled granulocytes reached a maximum in the peripheral blood (Fig. 4 B). It is known that BrdU labeling intensity is diluted by half with every cell division after BrdU incorporation. Consequently, by tracking the changes in relative BrdU intensity, we can determine how many division cycles the neutrophils from precusor cells have undergone. Cells in the BrdU^{bright} region correspond to granulocytes that incorporated BrdU in their last mitosis, whereas those in the BrdU^{dim} region have gone through one or more divisions after BrdU incorporation. As shown in Fig. 4 C, 40% of neutrophils were in the BrdU^{dim} pool in WT mice, whereas only 22% of neutrophils from ARKO mice were BrdU^{dim}, suggesting a markedly reduced mitotic cell division of neutrophil precursors in bone marrow of ARKO mice.

Granulocytes from bone marrow of ARKO mice are susceptible to apoptosis

To determine if neutropenia in ARKO mice is partly caused by neutrophil apoptosis, we examined the bone marrow cell

counted. 200-count manual leukocyte differentials were examined after Wright-Giemsa staining. Numbers of neutrophils and precursor cells were calculated by multiplying neutrophil differential ratios by the total green fluorescent cell count. Triplicate experiments were performed and the error bars represent the SD.

apoptosis using a FACS-based assay with Annexin V and 7-amino-actinomycin-D (AAD) staining. We did not observe a significant number of apoptotic Gr-1$^+$ cells in fresh bone marrow from either WT or ARKO mice (Fig. 5 A), which might be caused by rapid clearing of apoptotic cells by macrophages in vivo. We then examined survival of mature bone marrow neutrophils in vitro and found that 25% of ARKO neutrophils were apoptotic cells as compared with 19% in WT cells in culture without G-CSF treatment, indicating that ARKO neutrophils are moderately more susceptible to spontaneous apoptosis than WT cells (Fig. 5 B). On the other hand, with G-CSF treatment for 48 h, only 10% of WT neutrophils, but 20% of ARKO neutrophils, remained apoptotic (Fig. 5 B). These results suggest that G-CSF is unable to delay apoptosis in ARKO neutrophils.

Together, the proliferation and apoptosis assays suggest that neutropenia resulting from loss of AR might be caused by decreased proliferation of neutrophil precursors and increased apoptosis of neutrophils in bone marrow.

The response to G-CSF is impaired in granulocytes lacking AR

G-CSF–mediated apoptosis protection might be less effective in ARKO granulocytes because of impaired response to G-CSF. To investigate the granulopoietic response to G-CSF in

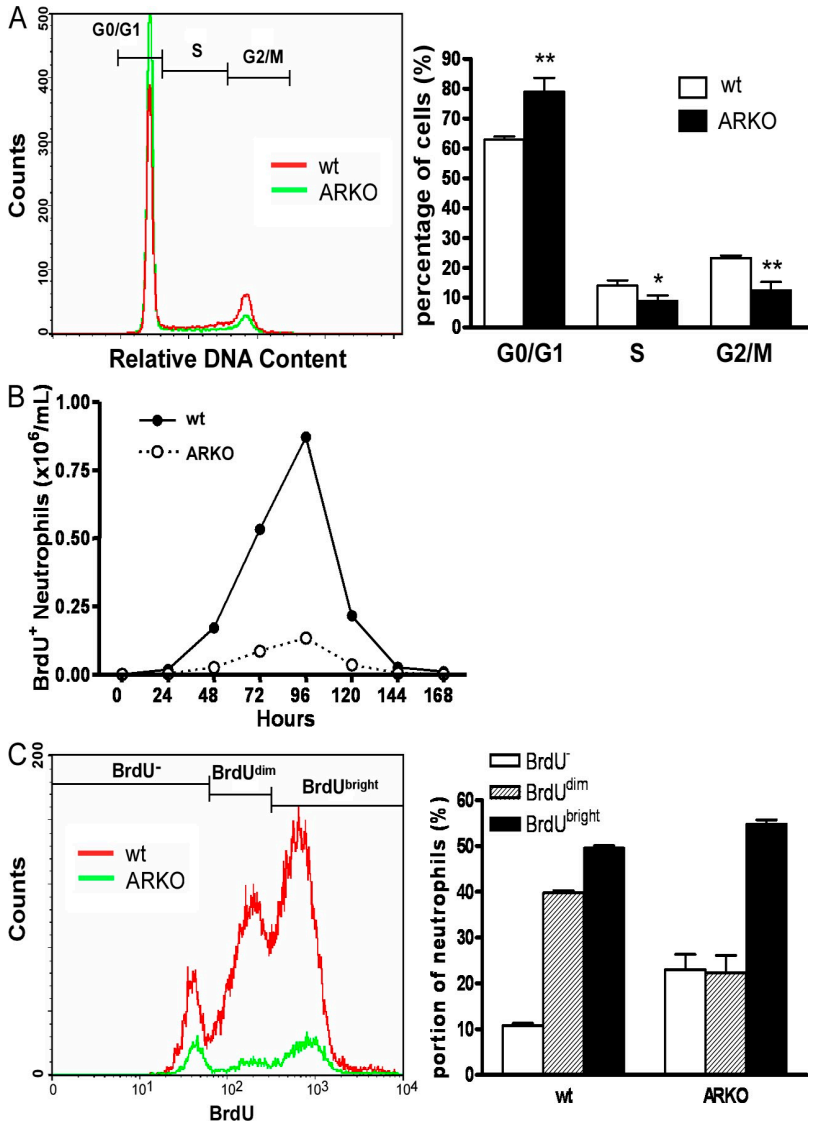

Figure 4. Proliferative potential of neutrophil precursor and progenitor cells. (A) Cell cycle analysis of total bone marrow Gr-1$^+$ cells from WT and ARKO mice. Comparison of cell cycle distributions shows that 9-wk-old ARKO mice have a lower percentage of cells in the S-phase and the G2/M phase of the cell cycle compared with WT littermates. Data are presented as the mean ± standard deviations (SD) of three independent experiments in the right panel. (B) Kinetics of BrdU labeled neutrophils in the blood of WT and ARKO mice after BrdU injection. (C) Comparison of BrdU incorporation in WT and ARKO blood neutrophils. At 96 h post injection, the ratio of BrdU^{dim} in blood neutrophils is lower in 9-wk-old AR-deficient mice (n = 4) as compared with WT littermates (n = 4). For each group, 10^5 cells from each of four mice were pooled and used for analysis. The results are presented as percentage of blood neutrophils from four-replicate experiments and the error bars represent the SD in the right panel.

WT and ARKO littermates, we monitored blood neutrophil counts with daily injections of G-CSF for 9 d (Fig. 5 C). We observed that ARKO mice had lower increasing rate of blood neutrophils in response to G-CSF as compared with WT mice. These results suggest that there might be an inhibition to G-CSF signaling in AR-deficit myeloid cells. Using real-time quantitative PCR (Q-PCR), we measured the mRNA expression of G-CSF–downstream target genes, such as SOCS3, flotillin, chemokine (C-C motif) receptor-like 2, glycerol kinase, and complement component 3a receptor 1,

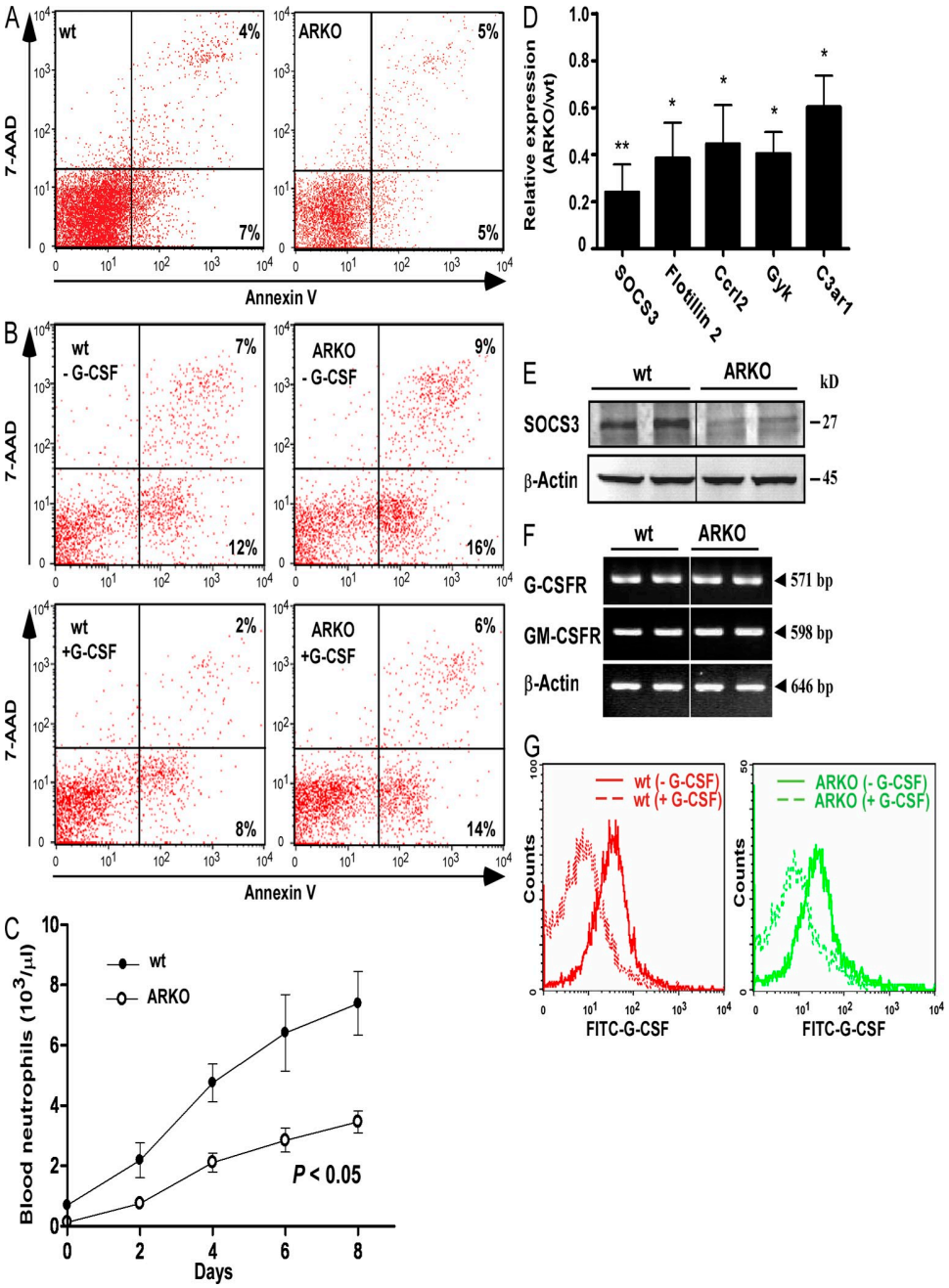

Figure 5. Insensitivity to G-CSF signaling in ARKO neutrophils. (A) Only few apoptotic neutrophils can be found in freshly isolated WT and ARKO bone marrow cells. (B) G-CSF protection against apoptosis in ARKO bone marrow neutrophils was less than in WT cells in vitro. Isolated mature bone marrow neutrophils were cultured in RPMI medium with 20% FCS without or with G-CSF (100 ng/ml) for 48 h. Neutrophils were then stained with Annexin V and 7-AAD, and analyzed by flow cytometry. (C) A lower increasing rate of blood neutrophils was found in ARKO mice in response to G-CSF injection. (D) G-CSF target genes are down-regulated in ARKO neutrophils. Data represent mean ± SD for three separate experiments. *, $P < 0.05$; **, $P < 0.01$. (E) SOCS3 protein expression is decreased in ARKO neutrophils. (F) mRNA expression of G-CSFR is comparable between WT and ARKO neutrophils. (G) G-CSF binding to WT and ARKO neutrophils is similar.

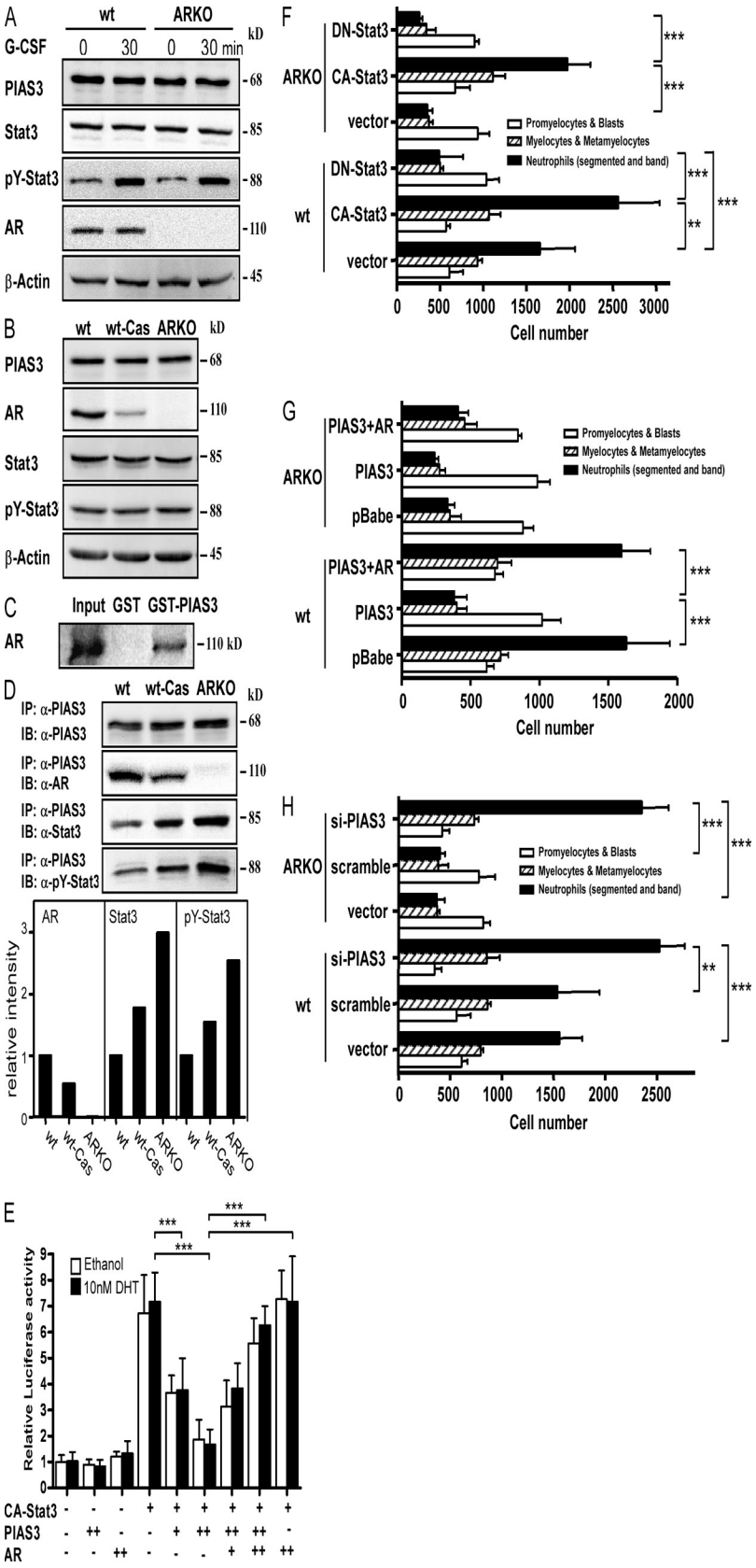

and found their mRNA expressions were decreased in ARKO granulocytes (Fig. 5 D). Protein expression of SOCS3, a major downstream target of G-CSF, was also significantly reduced (Fig. 5 E) in isolated bone marrow granulocytes from ARKO mice compared with those from WT littermates. These results suggest that G-CSF signaling could be suppressed in ARKO granulocytes. We then examined the expression of G-CSFR using semiquantitative RT-PCR and a flow cytometric–based G-CSF binding assay. We saw no difference in mRNA and surface protein expression of G-CSFR between granulocytes from ARKO and WT mice (Fig. 5, F and G).

Stat3 activity and ERK activation in G-CSF signaling are reduced in ARKO granulocytes

To investigate if downstream mediators of G-CSF signaling are suppressed by AR deficiency, we examined the expression of Stat3, a proximal mediator of the G-CSF signaling (34, 35). We found that the expression of both total Stat3 and the tyrosine-phosphorylated form of Stat3 (pY-Stat3) were similar between isolated bone marrow neutrophils from WT and those from ARKO mice in the absence or presence of G-CSF stimulation (Fig. 6 A). Similar levels of Stat3 and pY-Stat3 proteins were also observed in bone marrow neutrophils from castrated mice and those from WT and ARKO in the presence of G-CSF (Fig. 6 B). These results suggest that loss of AR does not influence the expression or the function of G-CSFR. Interestingly, we found that endogenous AR of granulocytes from castrated mice is less abundant (Fig. 6 B), which could be caused by the decrease of AR protein stability in the prolonged absence of androgen (36, 37). This is further supported by the finding that castration resulted in a significant reduction of AR expression and that exogenous DHT administration restored the reduced AR expression (38).

Because early studies have demonstrated that PIAS3 could inhibit Stat3 signaling via blocking Stat3 DNA binding (39), we sought to explore if AR interacts with PIAS3 and affects its inhibition on Stat3 activity. The glutathione *S*-transferase (GST) pull-down data shows that there is a direct protein–protein interaction between PIAS3 and AR (Fig. 6 C). The PIAS3 interaction with AR possibly occurs through the PIAS3 N terminus, which contains a LXXLL motif, an α-helical protein interaction module that mediates interactions between AR coregulators and AR. Using a coimmunoprecipitation assay, we found that anti-PIAS3 antibodies can precipitate more pY-Stat3 in granulocytes from ARKO, followed by that from castrated mice, which is more than that from WT mice (Fig. 6 D). This result suggests that loss of AR in ARKO granulocytes results in increased PIAS3-mediated sequestering of pY-Stat3, leading to the suppression of G-CSF signaling. A reporter assay further showed that suppression of constitutively active Stat3 (CA-Stat3) transactivation by PIAS3 was relieved by AR in a dose-dependent manner (Fig. 6 E). Notably, the major induction of Stat3 reporter is through increasing AR and is only slightly enhanced by adding androgen (Fig. 6 E), suggesting that androgen is not required for the AR's rescue of stat3 activity from the inhibition by PIAS3.

Stat3 activation has been demonstrated to promote differentiation of myeloid cell lines (34, 35, 40–43). To further investigate if increased activated Stat3 can rescue differentiation of ARKO myeloid progenitors, we infected primary bone marrow GMPs with retroviruses carrying CA-Stat3, dominant-negative Stat3 (DN-Stat3), or retroviruses carrying pMSCV vector alone. We seeded infected cells into methylcellulose medium in the presence of G-CSF, and harvested colonies after 7 d. WT and ARKO colonies infected with retroviruses carrying DN-Stat3 exhibited fewer mature neutrophils (Fig. 6 F). In contrast, WT and ARKO colonies infected with retroviruses expressing CA-Stat3 contained more mature neutrophils (Fig. 6 F). These results suggest that blocking endogenous Stat3 function by overexpression of DN-Stat3 could retard neutrophil differentiation, whereas increase of CA-Stat3 could rescue neutrophil differentiation.

To further explore the relationship between AR and PIAS3 in granulocytic differentiation, we examined differential counts of neutrophils in colonies infected with PIAS3 and PIAS3-siRNA. We infected primary WT and ARKO GMPs with retroviruses carrying PIAS3, PIAS3-siRNA, and controls. We then seeded infected cells into methylcellulose medium with G-CSF for 7 d, and then examined differential counts of fluorescent colony cells. We found PIAS3 overexpression reduced mature neutrophils, but increased AR could rescue the reduction (Fig. 6 G). We also found that PIAS3 knockdown by PIAS3-siRNA could restore mature neutrophil numbers in ARKO colonies (Fig. 6 H).

The binding of G-CSF to its receptor activates not only the Jak–Stat3 pathway (44) but also the Ras–Raf–ERK signaling cascade (45). No ERK1/2 activation was found in WT and ARKO neutrophils before G-CSF treatment (Fig. 7 A). We observed that ERK1/2 phosphorylation was significantly decreased in ARKO bone marrow granulocytes with G-CSF

Figure 6. Stat3 transcriptional activity is reduced in ARKO neutrophils. (A) PIAS3, Stat3, and pY-Stat3 proteins are comparable in WT and ARKO bone marrow neutrophils. Cells were isolated from mice and then incubated with G-CSF (40 ng/ml) at 37°C for the indicated period. (B) AR protein expression is lower in bone marrow neutrophils of castrated mice than those of WT mice, while Stat3 and pY-Stat3 levels are comparable. Bone marrow Gr-1$^+$ cells were isolated from mice and then incubated with G-CSF (40 ng/ml) at 37°C for 30 min. (C) AR interacts with the GST-PIAS3 in the GST pull-down assay. (D) Binding of Stat3 by PIAS3 is more in ARKO bone marrow neutrophils. The result of band intensities of Stat3, pY-Stat3, and AR in the coimmunoprecipitation experiment was normalized with band intensities of PIAS3 and shown in the right panel. (E) AR can relieve the PIAS3 inhibition of activated Stat3 action. The results are presented as fold induction of luciferase activity from triplicate experiments using CV-1 cells and the error bars represent the SD. ***, $P < 0.001$. (F) CA-Stat3 induces but DN-Stat3 inhibits neutrophil maturation. (G) PIAS3 inhibits neutrophil maturation, while increased AR rescues the inhibition. (H) PIAS3-siRNA increases neutrophil maturation. Results are presented as cell numbers of neutrophils and precursors from triplicate experiments and the error bars represent the SD. *, $P < 0.05$; **, $P < 0.01$; ***, $P < 0.001$.

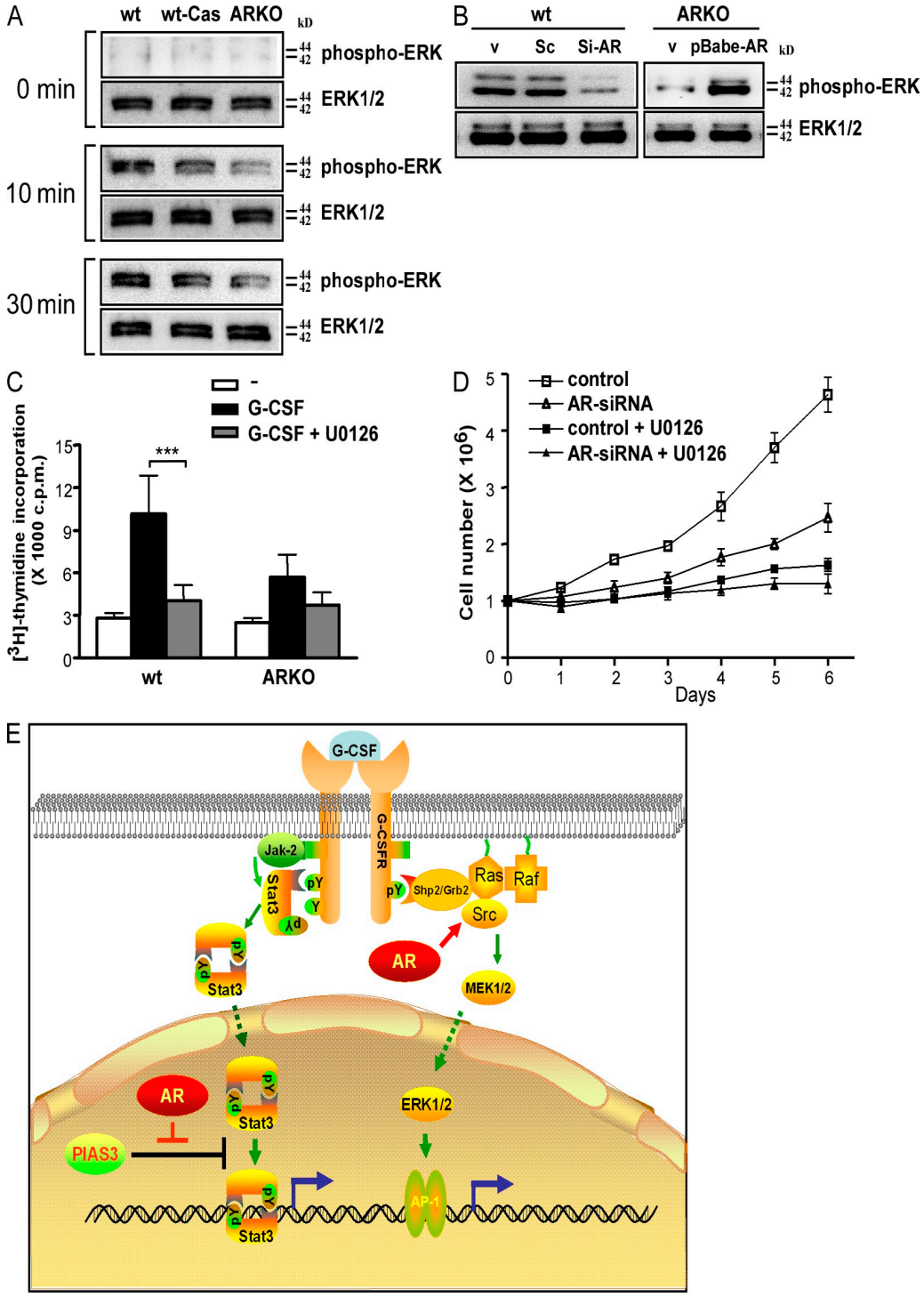

Figure 7. AR is essential for ERK1/2 activation in G-CSF induced neutrophil proliferation. (A) With G-CSF (40 ng/ml) treatment for the indicated times, ERK1/2 phosphorylation status was examined in bone marrow neutrophils of WT, castrated WT, and ARKO mice. (B) AR is required for G-CSF-induced ERK1/2 phosphorylation. By immunoblotting, the expression status of phosphorylated ERK1/2 and total ERK1/2 were compared among each group of G-CSF–induced granulocytes derived from WT or ARKO bone marrow cells infected with retroviruses carrying AR, AR-siRNA, or control vectors. v, vector alone; Sc, pSuperior-scrambled siRNA; Si-AR, pSuperior-AR siRNA. (C) U0126 almost abolishes G-CSF–induced proliferation of bone marrow cells. In the presence or absence of G-CSF (10 ng/ml), bone marrow cells (10^6/ml) were incubated with or without 1 μM U0126 for 3 d. Proliferative activity was then examined by ^{3}H-thymidine incorporation. (D) Effects of AR deficiency on the human myeloblastic cell line, KG-1. Stably transfected cells were plated at 5×10^5 cells/ml in RPMI medium and the number of total viable cells was calculated each day. Results are the mean of three independent experiments and the error bars represent the SD. (E) Schematic representation of the role of AR in G-CSF signaling.

treatment (Fig. 7 A). We then found that in the presence of G-CSF, there is a decrease in phosphorylated ERK1/2 in WT bone marrow cells carrying AR-siRNA, whereas exogenous AR promotes ERK1/2 activation in ARKO bone marrow cells (Fig. 7 B). Next, we examined the effects of AR deficiency on the G-CSF–induced proliferation of primary bone marrow cells and the human myeloblastic cell line KG-1. Compared with ARKO cells, WT bone marrow cells showed a significantly higher proliferative activity in response to G-CSF (Fig. 7 C). Similarly, under G-CSF treatment, WT KG-1 cells also showed higher cell proliferation than the KG-1 clone carrying hAR-siRNA (Fig. 7 D). Furthermore, we found that U0126 (MEK kinase inhibitor) abolished a large part of G-CSF-induced cell proliferation for those cells containing AR (Fig. 7 C and D). All of these results suggest that AR is essential for the G-CSF–induced ERK activation and subsequent granulocytic proliferation. It has been reported that AR is important for the activation of c-Src–Ras–Raf–ERK signaling cascade through the interaction between the proline-rich motif of AR and the SH3 domain of c-Src (11). Also, our previous studies have demonstrated that AR contributes to ERK activation in an androgen-independent manner (13).

Together, these results indicate that AR not only releases the PIAS3 inhibition of the Stat3 but also promotes ERK activation in G-CSF signaling (Fig. 7 E).

Granulocytes from ARKO mice are capable of phagocytosis and oxidative burst, but have reduced chemokine and cytokine production

We then asked if any functions of neutrophils derived from ARKO mice were impaired as compared with WT controls. First, we examined the oxidative burst and phagocytic activities of granulocytes derived from ARKO and WT mice by incubating granulocytes with fluorescein-labeled *Escherichia coli* at 37°C (Fig. 8 A). In addition, we assessed the oxidative burst in response to PMA, fMLP, or anaphylatoxin C5a stimulation by monitoring the production of H_2O_2, which converts 2′,7′-dichlorofluorescein acetate, a nonfluorescent precursor, to 2′,7′-dichlorofluorescein. The fluorescence intensity of 2′,7′-dichlorofluorescein was comparable in the WT and ARKO neutrophils as stimulated by PMA (Fig. 8 B), fMLP (Fig. S3), or C5a (Fig. S3), showing that the oxidative burst capacity of the two genotypes was similar. These results suggest that both phagocytosis and the oxidative burst are normal in granulocytes from ARKO mice.

Chemokines and cytokines are important for leukocyte migration and inflammatory response. To assess the expression of chemokines and proinflammatory cytokines in the current study, we used Q-PCR to measure the mRNA levels in WT and ARKO granulocytes. ARKO cells had lower levels of IL-1β, IL-6, TNF-α mRNA, and several chemokines than WT cells (Fig. 8 C), suggesting that reduced production of chemokines and proinflammatory cytokines might influence the functions of neutrophils or other leukocytes through autocrine or paracrine pathways.

ARKO neutrophils show reduced neutrophil migration in response to CXCR2 ligands, but exhibit normal neutrophil degranulation

The chemokine receptor CXCR2 plays an important role in neutrophil migration (46). Neutrophil chemoattractants macrophage-inflammatory protein-2 (MIP-2) and KC/CXCL1 can specifically bind to CXCR2, whereas fMLP signals through a different G protein–coupled receptor (47–50). To test the migration capability of ARKO neutrophils, we examined the chemotactic response toward MIP-2, KC, and fMLP. As shown in Fig. 8 D, ARKO neutrophils demonstrated reduced migration activities toward the chemoattractants MIP-2 and KC compared with WT cells; however, ARKO and WT neutrophils had similar responses to fMLP. It has been shown that lack of Stat3 can impair CXCR2-dependent neutrophil migration (51), and our results are correlated with that finding because the Stat3 activity is mostly inhibited in ARKO neutrophils.

We then examined the release of β-glucuronidase and lactoferrin as the markers of primary and secondary granules from isolated mature neutrophils after stimulation. We found that WT and ARKO neutrophils showed no differences in the release of β-glucuronidase or lactoferrin induced by fMLP, C5a, and PMA (Fig. 8 E).

ARKO mice are more susceptible to microbial infection

To explore if neutropenic ARKO mice have impaired host resistance to acute bacterial infection, we injected 9-wk-old ARKO mice and age-matched WT controls (10 animals per group) intraperitoneally with a virulent strain of *E. coli*. Survival of the mice was monitored over 60 h. At 12 h after injection, all 10 ARKO mice showed signs of severe infection, including diarrhea, hunchback, imbalance, ruffled fur, and eye infection, but only 3 out of 10 WT mice exhibited signs of infection (Fig. 8 F). Moreover, all 10 ARKO mice were dead within 36 h, and only 1 WT mouse died within that time frame (Fig. 8 G). All remaining WT mice were still alive at 60 h. The inability of the ARKO mice to survive the *E. coli* challenge shows that these animals are more susceptible than WT controls to bacterial infection.

DISCUSSION

It is interesting that neutropenia was observed in ARKO and Tfm mice, whereas castrated male mice only have moderate reduction of neutrophil counts in both blood and bone marrow (Fig. 2, C–E), suggesting that AR, but not androgen, is critical for neutrophil homeostasis. Other evidences to support our hypothesis include the following: (a) Exogenous androgen can restore neutrophil counts in castrated WT mice, but not ARKO mice (Fig. 2, C–E). (2) Female ARKO mice have neutropenia, but WT female mice, with 10-fold less androgen levels compared with male, still maintain normal neutrophil counts (Fig. 1 H). (3) Our mechanistic studies indicate that AR reduces the inhibition of PIAS3 to Stat3 transcriptional activity, and adding androgen only mildly enhances the AR effect on Stat3 signaling (Fig. 6 E). (4) Without adding androgen, AR overexpression still increases granulocytic differentiation

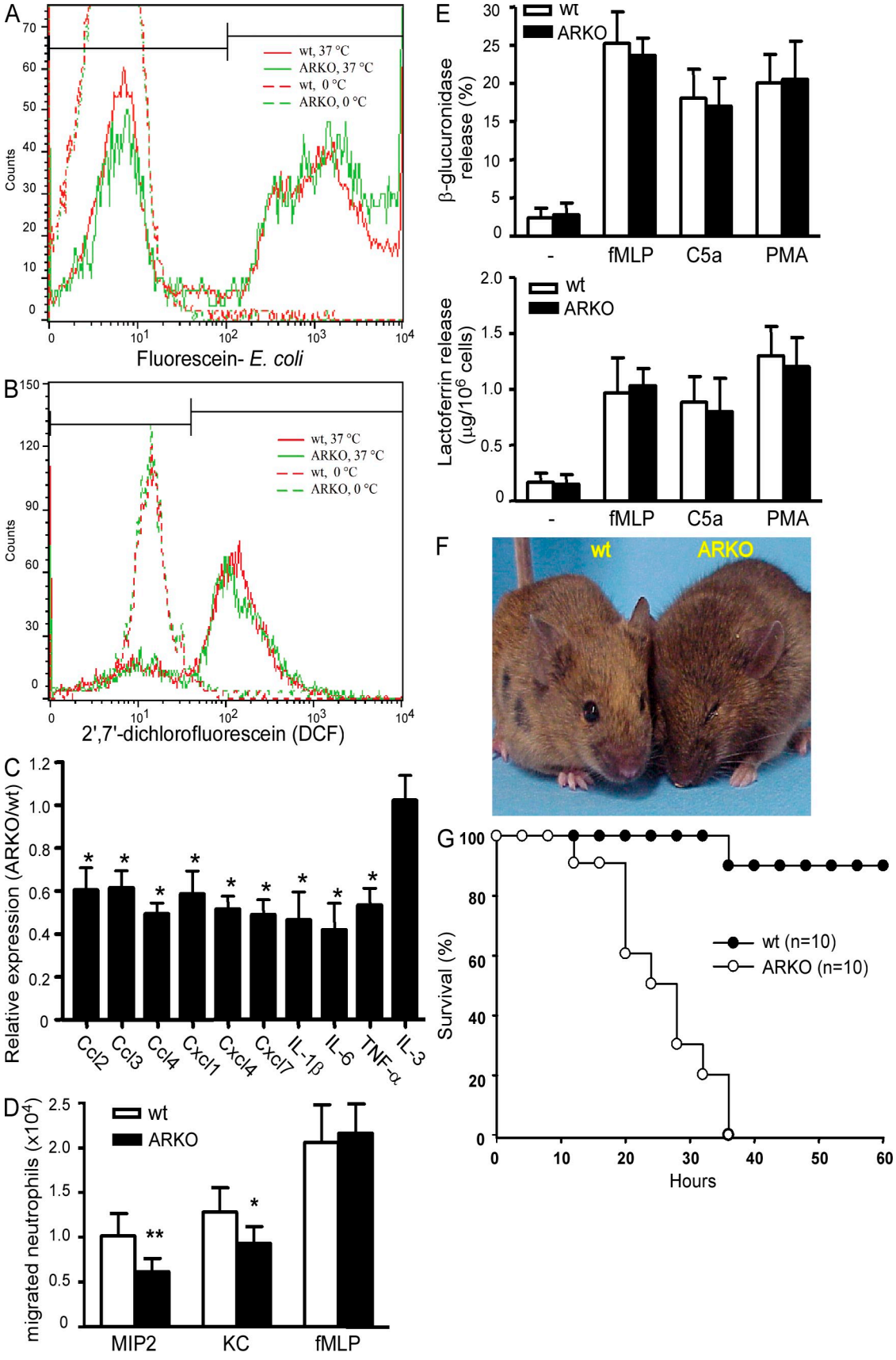

in colony formation assays (Fig. 3 E). With these observations, we believe that AR confers a direct and more profound effect than androgen. We note with interest that neutropenia resulting from AR ablation contrasts with the effect of knocking out the estrogen receptor β. The estrogen receptor β KO mice show an overproduction of mature granulocytes (52). These opposing effects on granulopoiesis suggest that both AR and ER are required to maintain neutrophil homeostasis.

In vitro and transgenic mouse studies have demonstrated that Stat3 plays an essential role in G-CSF–dependent granulopoiesis (35, 51, 53–56). Moreover, several reports have shown that SOCS3 KO mice, in which Stat3 activity is persistent, developed severe neutrophilia (57–59). Paradoxically, mice with targeted deletion of the Stat3 gene in hematopoietic cells were also found to develop neutrophilia (60–63). Nevertheless, ERK1/2 hyperphosphorylation was found in bone marrow cells of Stat3 conditional KO mice, and it has been shown to contribute to neutrophilia in those animals (63). It is possible that the ERK1/2 hyperactivation results from SHP–Grb2–Src binding to available Stat3 docking sites on G-CSF receptor and overactivating the Ras–Raf–ERK signaling cascade. This possible signal crossover has been suggested in some reports showing that G-CSFR truncated mutants lacking the receptor C terminus, which contains tyrosine Y764 (the default docking site for SHP-2/Grb2), still have the ability to activate p21Ras via the SHP/Grb2 route linked to Y704 (the stat3 docking site) of the G-CSFR (41, 64). Clearly, further investigation is still required to determine the precise role of Stat3 in neutrophil development.

Several KO models have been established for genes involved in the regulation of myelopoiesis. C/EBPα$^{-/-}$ mice have circulating myeloblast-like cells but lack mature neutrophils in vivo at birth. Although it was found that a lower PU.1:C/EBPα ratio directs granulocytic differentiation over macrophage differentiation in myeloid cell fate determination, a PU.1$^{-/-}$ mice study demonstrated that PU.1 is not essential for neutrophil lineage commitment, but is necessary for normal development, maturation, and function of neutrophils. Gfi$^{-/-}$ mice are severely neutropenic and accumulate immature monocytic cells in blood and bone marrow. We found the mRNA levels of PU.1, C/EBPα, and Gfi in ARKO bone marrow neutrophils are comparable to those detected in WT neutrophils (unpublished data), indicating that C/EBPα, PU.1, and Gfi might not account for the granulopoietic defect observed in ARKO mice. Notably, a few mature neutrophils can still be observed in G-CSF$^{-/-}$, G-CSFR$^{-/-}$, and G-CSF$^{-/-}$GM-CSF$^{-/-}$M-CSF$^{-/-}$ mice (5, 65, 66), suggesting that a myeloid-CSF independent mechanism exists in basal granulopoiesis. It might be interesting to further study whether AR also modulates a myeloid–CSF-independent pathway.

Androgens can stimulate erythropoiesis and have been used clinically for treatment of aplastic anemia (26, 27). However, our data (Table I A) indicate that red blood cell numbers and hemoglobin levels in WT and ARKO mice are similar, suggesting that AR is not required for steady-state erythrocyte production under physiological conditions. These results, however, are at odds with early reports showing that androgens could stimulate erythropoiesis (67). The diverse effect on erythropoiesis by different androgen derivatives is indicative of the complexity of androgen control in erythropoiesis. 5α-DHT binds to the AR and might stimulate erythropoiesis indirectly by increasing levels of erythropoietin, whereas 5β epimers (5β-DHT and etiocholanolone) do not bind to the AR, yet effectively increase the number of erythropoietic progenitor cells, thereby also enhancing erythropoiesis (68–73). It will be interesting to study if androgen stimulates erythropoiesis through an AR-independent pathway.

In summary, the data presented here indicate AR is essential for steady-state granulopoiesis. Further studies that explore potential cross talk between AR and other myeloid regulators in granulopoiesis might help reveal a better understanding of how cell signaling networks tightly control neutrophil homeostasis.

MATERIALS AND METHODS

Mice. Construction of targeting vectors and generation of the chimera founder mice have been previously described (12). The original strain background of the mosaic founder mice was C57BL6/129sv. We have generated floxed AR mice with a nearly pure C57BL/6 background by backcrossing the original C57BL6/129sv background floxed AR mice with pure C57BL/6 background mice for more than eight generations. β-Actin is constitutively and ubiquitously expressed; thus, the β-actin promoter-driven Cre (ACTB-Cre, FVB background; The Jackson Laboratory) will express and delete floxed AR fragments in all the tissues. WT and ARKO mice were genotyped

Figure 8. Neutrophil function and host defense against infection in the absence of AR. (A) Uptake of fluorescein-labeled *E. coli* by WT and ARKO neutrophils at 37°C. (B) Flow cytometric analysis of oxidant production and subsequent 2′,7′-dichlorofluorescein generation in WT and ARKO granulocytes after PMA stimulation. (C) Relative mRNA expression of chemokines and cytokines in isolated WT and ARKO bone marrow granulocytes. *, $P < 0.05$. (D) Mature bone marrow neutrophils from WT or ARKO mice were tested for migration in Transwell chambers toward the indicated chemoattractant (200 ng/ml MIP-2, 1 µg/ml KC, or 100 µM fMLP). The number of cells migrated through the Transwell was determined by cell counting. Data from six independent experiments are presented and the error bars represent the SD. *, $P < 0.05$; **, $P < 0.01$. (E) Neutrophil degranulation of WT and ARKO neutrophils was examined without or with stimulation by fMLP, C5a, or PMA. (top) The release of the primary granules was examined using the β-glucuronidase activity in the supernatant of stimulated neutrophils. Data are presented as the percentage of total cellular β-glucuronidase content. (bottom) Release of the specific granule marker lactoferrin in the supernatant of stimulated neutrophils was quantified by ELISA. Both degranulation assays were performed in six independent experiments. (F) Representative photograph of WT and ARKO mice after 12-h intraperitoneal injection with *E. coli*. ARKO mice showed signs of severe infection, such as hunchback, ruffled fur, and eye infection; however, WT mice remained normal. (G) Kaplan-Meier survival curve of WT and ARKO mice in response to intraperitoneal challenge with *E. coli*. We examined the time course of survival following *E. coli* infection. Survival over time is shown as percentage mice remaining.

by PCR, as described previously (12). Male Tfm and WT control mice (C57BL/6J-A-Ta[6J]$^{+/Y}$) were purchased from The Jackson Laboratory. All animal experiments were approved by the University Committee on Animal Resources of the University of Rochester.

Castration. Castration was performed under anesthesia using sterile instruments and gloves. A transverse scrotal incision was made, the testicles were exposed, the vas deferens and spermatic blood vessels were ligated, and the testicles were removed. A sham operation was performed for noncastrated controls in which the testis and epididymis were only pulled out and then returned to the scrotum. The scrotal incision was closed using a single skin clip. Animals were placed in a clean cage and monitored until fully recovered from anesthesia.

Androgen supplementation. Androgen supplementation in castrated WT mice and ARKO littermates was achieved by subcutaneous implantation of 60-d time-release pellets (Innovative Research of America) containing DHT (5 mg per pellet); mice were sacrificed 14 d after androgen supplementation. The levels of plasma DHT were determined by a DHT ELISA Kit (Alpha Diagnostic International) according to the manufacturer's protocol.

Blood and bone marrow sampling. Between 6 a.m. and 8 a.m., we collected peripheral blood through cardiac puncture using a heparinized 3-ml syringe with a 30-gauge needle on mice under anesthesia. We dissected the femur free from the muscle, and then cut both at the knee and hip for removal. We removed bone marrow from each femur by flushing with 1 ml RPMI 1640 (using a 26-gauge needle and a 1-ml syringe) into a single well of a 6-well culture plate.

Cytology and automated hematology analysis. Bone marrow smears, blood smears, and cytospin preparations were stained with Wright-Giemsa for morphological assessment and manual differential counting. Hematologic parameters from blood samples obtained from 8–12-wk-old mice were measured using an Abbot CELL-DYN 4000 system.

Cell isolation. We isolated neutrophils from bone marrow or peripheral blood by using the EasySep selection kit (StemCell Technologies) according to the manufacturer's suggested procedures. Mature bone marrow neutrophils were isolated by discontinuous Percoll density gradient centrifugation.

Cell staining and FACS analysis. 1–5 × 10^5 cells were incubated on ice for 30 min with saturating amounts of antibody. Cells were washed with ice-cold PBS containing 2% fetal bovine serum, and flow cytometric analyses were performed using a dual-laser FACSCalibur flow cytometer (BD). For analysis of white blood cell populations, we set gates to include those cells that were CD45$^+$ and viable by FSC and SSC scan profiles. Neutrophils were stained by fluorochrome-conjugated, neutrophil-specific monoclonal antibodies (clone 7/4; Invitrogen) or anti–Gr-1 antibodies (clone RB6-8C5; eBioscience). For intracellular AR staining, after cells were incubated with fixative buffer (2% paraformaldehyde) and permeabilized with permeabilization solution (0.1% saponin in PBS containing 2% fetal bovine serum), intracellular AR was stained by anti-AR antibody (clone C-19; Santa Cruz Biotechnology, Inc.), followed by fluorochrome-conjugated anti–rabbit IgG antibodies. Data were collected and analyzed from at least 10,000 gated events using CellQuest software (BD). To assess surface G-CSFR expression, G-CSF was biotinylated. Bone marrow Gr-1$^+$ cells were incubated at 48°C for 1 h with biotinylated G-CSF (25 ng per 10^6 cells) in the presence or absence of a 100-fold molar excess of nonlabeled G-CSF, followed by incubation with FITC-conjugated streptavidin. All cells were analyzed on a FACSCalibur flow cytometer.

Neutrophil differential counts in humans before and after androgen ablation. We collaborated with the Department of Urology at the Sir Run Run Shaw Hospital to collect blood analysis data from each patient before and after surgical castration (0–2 wk before castration and 2–4 wk after castration). Appropriate data excluded any patients receiving radiation therapy and/or chemotherapy. Diurnal rhythms of neutrophil counts and possible increased neutrophil counts from smoking and infections were also prevented, and the results are statistically analyzed. We requested coded data from chart reviews that include only patient diagnosis, treatments, time of blood drawn, and blood analysis data.

FACS detection of BrdU-labeled neutrophils, cell cycle analysis, and apoptosis assays. The immunofluorescent staining of intracellular BrdU incorporation has been previously described (74). To study cycling status of granulocytes, we first stained bone marrow cells with FITC-Gr-1 antibody, fixed cells in 70% ethanol and removed residual RNA by RNase A, and then further stained them with propidium iodide (final concentration 5 μg/ml) for analysis by a FACSCalibur flow cytometer. Data were further analyzed using CellQuest Software (BD) for DNA histogram analysis of Gr-1$^+$ cells. For neutrophil apoptosis assays, bone marrow cells were stained with Annexin-V and 7-AAD. High-SSC cell population was then gated for apoptosis analysis.

Hematopoietic progenitor cell assay. Single-cell suspensions of bone marrow (2.5 × 10^4 cells) in methylcellulose medium (MethoCult M3234, Stem Cell Technologies) were plated in 35-mm Petri dishes in triplicate and incubated at 37°C. Purified recombinant murine (rm)G-CSF (10 ng/ml), rmGM-CSF (10 ng/ml), rmM-CSF (10 ng/ml), rmIL-3 (10 ng/ml), and rmIL-6 (400 ng/ml) (R&D Systems) were used.

RNA analysis. Neutrophils were isolated by EasySep selection kit (Stem Cell Technologies) and total RNA was extracted from cells using TRIzol reagent (Invitrogen). We performed reverse transcription using Superscript II reverse transcription and oligo-dT primers (Invitrogen) on 250 ng of total RNA. In semiquantitative RT-PCR, cDNA was diluted 5, 25, 50, and 100 times, and an aliquot (2 μl) of the reverse transcription reaction was subjected to PCR in a thermocycler (MyCycler; BioRad Laboratories). β-Actin was used as an internal control. Q-PCR was performed in a final volume of 25 μl containing 1 μg cDNA, 12.5 μl SYBR Green Mix (2X), 6 pmol of each primer set. The primer sequences for Q-PCR are listed in Table S1. The reaction mixtures were incubated on a iCycler (BioRad Laboratories) real-time PCR amplifier (BioRad Laboratories) programmed at 50°C, 2 min; 95°C 10 min; then 40 cycles for three steps at 95°C, 15 s to 60°C, 30 s to 72°C, 30 s; and finally at 70°C for 10 min. HPRT mRNA was used as the internal control. Real-time Q-PCR was performed by determining the cycle at which the abundance of the accumulated PCR product crosses a specific threshold, the threshold cycle (CT) in each reaction. The difference in average CT values between the internal control and a specific gene was calculated for each individual and termed ΔCT, which is comparable to the log-transformed, normalized mRNA abundance. For each gene, at least three samples with triplicate amplifications were performed and mean ± SD taken for data analysis.

Construction. The retroviral vectors pBabe-AR and pBabe-PIAS3 were constructed by ligating digested PCR products of AR and PIAS3 cDNA into a pBabe vector containing the SV40 promoter-driven GFP. To generate vectors for siRNA expression, the pSuperior-GFP-neo vector (OligoEngine) was digested and the annealed oligonucleotides were ligated into the vector. The nucleotide sequences for targeting mouse AR, PIAS3, and Stat3 were designed as 5′-TCTAGCCTCAATGAGCTTG-3′, 5′-GCCACTGCCCTTCTATGAA-3′, and 5′-AGCCGATCTAGGCAGATG-3′, respectively. Scrambled control shRNA unrelated to AR, PIAS3, and Stat3 sequences were used as negative controls. hAR-siRNA was described previously (13).

Isolation of GMP precursor cells. The myeloid-committed precursor populations from murine bone marrow were isolated by first depleting lineage marker–positive cells by means of immunomagnetic beads. The remaining cells were then stained with goat anti–rat immunoglobulin Texas red and anti–c-kit–APC and then enrichment sorted for Lin$^-$ c-kit$^+$ cells. The enrichment-sorted cells were then stained with anti-FcRII/III (CD16/32)–FITC, anti–c-kit–APC, anti–IL-7R–Alexa Fluor 594, anti–Sca-1–Alexa Fluor 594, and anti–CD34-biotin, followed by PE-avidin. The

GMP precursor population was sorted as Lin^- $CD16/32^+$ $CD34^+$ c-kit^+ $Sca\text{-}1^-$ $IL\text{-}7R^-$ cells.

Retroviral infection. Phoenix ectrophic cells were grown in DME supplemented with 10% FCS. Cells were typically seeded in 60-mm-diam plates at a density of 2.4×10^6 cells per plate and allowed to settle for 18 to 24 h. Cells were transfected with 5–10 μg of plasmid DNA using calcium phosphate transfection. The media containing the plasmid DNA precipitate were replaced with fresh media 16 h after transfection. Retroviral supernatants were collected 48 h after transfection from Phoenix cells transfected with the retroviral vector–based constructs and used to infect freshly sorted GMP precursor cells. Infections were performed with 1 ml of undiluted supernatant in 2 ml of DME plus 400 μg of Polybrene per ml at 37°C. After 4 h of incubation, 2 ml of DME with 10% FCS were added and incubated for an additional 20 h.

Green fluorescent colony formation and differentiation counting. After retroviral infection, single-cell suspensions of GMP precursor cells in methylcellulose medium (MethoCult M3234; StemCell Technologies Inc.) were plated in 35-mm culture dishes in triplicate and incubated at 37°C in the presence of rm G-CSF (10 ng/ml) in a humidified incubator maintained at 5% CO_2. After 7 d in culture, the numbers of green fluorescent colonies in each dish were counted, and green fluorescent colony cells were collected in suspension for cell counting. Cells were cytocentrifuged onto a microscope slide and stained with Wright-Giemsa for morphological assessment and 200-count manual differential counting.

In vivo administration of G-CSF. We injected three pairs of WT and ARKO littermates subcutaneously with rmG-CSF at 40 ng/g mice from day 0–8, and then examined blood neutrophil counts 4 h after G-CSF injection at the indicated days.

Reporter gene assays. CV-1 cells were transfected with 4 × IRF-LUC (1.5 μg) together with CA-Stat3 (0.5 μg), flag-PIAS3 expression construct (0.5 or 1.0 μg), and increasing amounts of AR (0.5 or 1.0 μg) with plasmid amount balance. The media was changed 2 h after transfection, and cells were cultured in media containing 10% charcoal depleted-FBS for 24 h, followed by treatment with or without 10 nM DHT for another 16–18 h. 5 ng phRL-TK per well was used as internal control. Cells were harvested, and the Luc activity was analyzed using Dual-Luc Reporter Assay System (Promega).

Immunoblot analysis of cells infected with retroviruses. We infected WT and ARKO GMPs or bone marrow cells with retroviruses carrying pBabe-AR, AR-siRNA, or controls. After retroviral infection, single-cell suspensions of bone marrow cells in methylcellulose medium were plated in culture dishes and incubated at 37°C in the presence of G-CSF (10 ng/ml). After 7 to 10 d in culture, colony cells were collected and further incubated with or without G-CSF (40 ng/ml) for 30 min, and cells were harvested for immunoblot analysis.

Immunoprecipitation. Cells were lysed in lysis buffer (50 mM Tris–HCl, pH 7.4, 0.3 M NaCl containing 1% NP-40, 1 mM sodium orthovanadate, 1 mM phenylmethylsulfonyl fluoride, and 10 μg/ml each of aprotinin, pepstatin, and leupeptin). Cell lysates were immunoprecipitated with anti-PIAS3 antibody as indicated. The immunoprecipitates from cell lysates were resolved on 5–20% SDS–PAGE and transferred to Immobilon membrane (Millipore). The membranes were then probed with each antibody as indicated. Immunoreactive proteins were visualized using an enhanced chemiluminescence detection system (GE Healthcare) and analyzed using Quantity One software (BioRad Laboratories).

GST pull-down assay. GST-PIAS3 fusion protein and GST protein were obtained by transforming expressing plasmids into BL21 (DE3) pLysS strain-competent cells followed with 1 mM isopropyl-D-thiogalactoside induction. GST fusion proteins were then purified by glutathione–Sepharose 4B as instructed by the manufacturer (GE Healthcare). In vitro translated [^{35}S]methionine-labeled proteins (2 μl) generated with the TNT-coupled reticulocyte lysate system (Promega) were mixed with the glutathione–Sepharose-bound GST proteins at 4°C for 3 h to perform the pull-down assay. The bound proteins were separated on a 10% or 15% SDS-polyacrylamide gel and visualized by PhosphorImager (GE Healthcare).

In vitro proliferative activity. In the presence or absence of G-CSF (10 ng/ml), bone marrow mononuclear cells (10^6/ml) were incubated in RPMI with or without U0126 (20 μM). After 3 d, 0.5 μCi ^{3}H-thymidine was added and the cells were cultured for an additional 8 h. Proliferative activity was then determined by ^{3}H-thymidine incorporation.

Assessment of phagocytosis and oxidative burst assays. Heparinized blood was incubated with opsonized fluorescein-labeled *E. coli* (Invitrogen) either at 37°C or at 0°C (control) for 10 min. After erythrocyte lysis, cells were washed twice and then stained with CyChrome–anti-Gr-1 antibodies. Oxidative burst in response to PMA was evaluated by detecting the intracellular conversion of dichlorofluorescein diacetate (DCFH-DA) to 2′,7′-dichlorofluorescein by flow cytometry. Leukocytes were stained with CyChrome–anti-Gr-1 antibodies and cells were mixed with 10 μM DCFH-DA and 10 nM PMA for 5 min at 37°C. We examined intracellular 2′,7′ dichlorofluorescein content in WT and ARKO $Gr\text{-}1^+$ cells. 10,000 gated $Gr\text{-}1^+$ cells were analyzed using CellQuest software. We isolated fresh mature bone marrow neutrophils by discontinuous Percoll density gradient centrifugation to perform oxidative burst assays in response to fMLP (1 μM) or C5a (1 μg/ml).

Neutrophil migration. Fresh WT and ARKO mature bone marrow neutrophils were obtained by discontinuous Percoll density gradient centrifugation. Neutrophils (5×10^5 cells) were then plated in 3 μm Transwells (Corning) with the indicated chemoattractant (200 ng/ml MIP-2, 1 μg/ml KC, or 0.1 mM fMLP) in the lower chamber. The number of cells migrated through the Transwell was determined by cell counting after incubation for 2 h at 37°C. Over 90% neutrophils remained viable at the end of the assay as judged by trypan blue exclusion.

Neutrophil degranulation. Cells (10^6/ml) were preincubated with 5 μg/ml cytochalasin B for 10 min and then stimulated with 1 μM fMLP, 0.5 μg/ml C5a, or 200 nM PMA for 20 min at 37°C. Reactions were stopped by cooling on ice and cell suspensions were centrifuged. β-Glucuronidase activity in supernatants of activated cells was measured spectrophotometrically using 4-methylumbelliferyl-β-d-glucuronide as substrate (75). β-Glucuronidase release is presented as the percentage of total cellular content. The secondary granule marker lactoferrin was determined by ELISA using anti-lactoferrin antibody (Sigma-Aldrich).

Survival after intraperitoneal infection. 10 WT and 10 ARKO mice were administered 5×10^5 colony forming units of *E. coli* (Serotype O18ac: K1:H7; American Type Culture Collection) by intraperitoneal injection and were followed for survival over 60 h.

Statistical analysis. Data are presented as the mean ± SD from at least three experiments, and statistical analysis was performed by either two-tailed Student's *t* test or one-way analysis of variance. The statistical significance of differences was set at $P < 0.05$.

Online supplemental material. Fig. S1 shows AR activity is knocked down by AR siRNA and restored by AR cDNA using retroviral infection in CV-1 cells. Fig. S2 shows AR-targeted disruption in colony cells derived from GMPs infected with retrovirus carrying AR-siRNA. Fig. S3 demonstrates that the oxidative burst induced by fMLP or C5a in WT and ARKO neutrophils was comparable. Table S1 shows primer sequences for Q-PCR analysis. Online supplemental material is available at http://www.jem.org/cgi/content/full/jem.20082521/DC1.

The authors are grateful to Karen Wolf and Leroy Hanchett for manuscript preparation and thank Marshall Lichtman, James Palis, Stephen Welle, and

Alexandra Livingstone for critical review. We thank Ke Shuai and Daniel Link for sharing PIAS3, 4 × IRF-Luc, pMSCV-Stat3C (CA-Stat3), and pMSCV-Stat3D (DN-Stat3) plasmids. This work was supported by National Institutes of Health Grant DK073414 and the George Whipple Professorship Endorsement.

The authors have no conflicting financial interests.

Submitted: 6 November 2008
Accepted: 13 April 2009

REFERENCES

1. Demetri, G.D., and J.D. Griffin. 1991. Granulocyte colony-stimulating factor and its receptor. *Blood*. 78:2791–2808.
2. Souza, L.M., T.C. Boone, J. Gabrilove, P.H. Lai, K.M. Zsebo, D.C. Murdock, V.R. Chazin, J. Bruszewski, H. Lu, K.K. Chen, et al. 1986. Recombinant human granulocyte colony-stimulating factor: effects on normal and leukemic myeloid cells. *Science*. 232:61–65.
3. Rex, J.H., S.C. Bhalla, D.M. Cohen, J.P. Hester, S.E. Vartivarian, and E.J. Anaissie. 1995. Protection of human polymorphonuclear leukocyte function from the deleterious effects of isolation, irradiation, and storage by interferon-gamma and granulocyte-colony-stimulating factor. *Transfusion*. 35:605–611.
4. Lord, B.I., M.H. Bronchud, S. Owens, J. Chang, A. Howell, L. Souza, and T.M. Dexter. 1989. The kinetics of human granulopoiesis following treatment with granulocyte colony-stimulating factor in vivo. *Proc. Natl. Acad. Sci. USA*. 86:9499–9503.
5. Lieschke, G.J., D. Grail, G. Hodgson, D. Metcalf, E. Stanley, C. Cheers, K.J. Fowler, S. Basu, Y.F. Zhan, and A.R. Dunn. 1994. Mice lacking granulocyte colony-stimulating factor have chronic neutropenia, granulocyte and macrophage progenitor cell deficiency, and impaired neutrophil mobilization. *Blood*. 84:1737–1746.
6. Nazareth, L.V., and N.L. Weigel. 1996. Activation of the human androgen receptor through a protein kinase A signaling pathway. *J. Biol. Chem*. 271:19900–19907.
7. Culig, Z., A. Hobisch, M.V. Cronauer, C. Radmayr, J. Trapman, A. Hittmair, G. Bartsch, and H. Klocker. 1994. Androgen receptor activation in prostatic tumor cell lines by insulin-like growth factor-I, keratinocyte growth factor, and epidermal growth factor. *Cancer Res*. 54:5474–5478.
8. Yeh, S., H.K. Lin, H.Y. Kang, T.H. Thin, M.F. Lin, and C. Chang. 1999. From HER2/Neu signal cascade to androgen receptor and its coactivators: a novel pathway by induction of androgen target genes through MAP kinase in prostate cancer cells. *Proc. Natl. Acad. Sci. USA*. 96:5458–5463.
9. Xie, Y., D.W. Wolff, M.F. Lin, and Y. Tu. 2007. Vasoactive intestinal peptide transactivates the androgen receptor through a protein kinase A-dependent extracellular signal-regulated kinase pathway in prostate cancer LNCaP cells. *Mol. Pharmacol*. 72:73–85.
10. Kasbohm, E.A., R. Guo, C.W. Yowell, G. Bagchi, P. Kelly, P. Arora, P.J. Casey, and Y. Daaka. 2005. Androgen receptor activation by G(s) signaling in prostate cancer cells. *J. Biol. Chem*. 280:11583–11589.
11. Migliaccio, A., G. Castoria, M. Di Domenico, A. de Falco, A. Bilancio, M. Lombardi, M.V. Barone, D. Ametrano, M.S. Zannini, C. Abbondanza, and F. Auricchio. 2000. Steroid-induced androgen receptor-oestradiol receptor beta-Src complex triggers prostate cancer cell proliferation. *EMBO J*. 19:5406–5417.
12. Yeh, S., M.Y. Tsai, Q. Xu, X.M. Mu, H. Lardy, K.E. Huang, H. Lin, S.D. Yeh, S. Altuwaijri, X. Zhou, et al. 2002. Generation and characterization of androgen receptor knockout (ARKO) mice: an in vivo model for the study of androgen functions in selective tissues. *Proc. Natl. Acad. Sci. USA*. 99:13498–13503.
13. Yeh, S., Y.C. Hu, P.H. Wang, C. Xie, Q. Xu, M.Y. Tsai, Z. Dong, R.S. Wang, T.H. Lee, and C. Chang. 2003. Abnormal mammary gland development and growth retardation in female mice and MCF7 breast cancer cells lacking androgen receptor. *J. Exp. Med*. 198:1899–1908.
14. Hu, Y.C., P.H. Wang, S. Yeh, R.S. Wang, C. Xie, Q. Xu, X. Zhou, H.T. Chao, M.Y. Tsai, and C. Chang. 2004. Subfertility and defective folliculogenesis in female mice lacking androgen receptor. *Proc. Natl. Acad. Sci. USA*. 101:11209–11214.
15. Matsumoto, T., H. Shiina, H. Kawano, T. Sato, and S. Kato. 2008. Androgen receptor functions in male and female physiology. *J. Steroid Biochem. Mol. Biol*. 109:236–241.
16. Mantalaris, A., N. Panoskaltsis, Y. Sakai, P. Bourne, C. Chang, E.M. Messing, and J.H. Wu. 2001. Localization of androgen receptor expression in human bone marrow. *J. Pathol*. 193:361–366.
17. Byron, J.W. 1970. Effect of steroids on the cycling of haemopoietic stem cells. *Nature*. 228:1204.
18. Resegotti, L., C. Dolci, L. Bertero, A. Genovese, F. Podesta, and D. Testa. 1981. Treatment of aplastic anaemia with methenolone, stanozolol and nandrolone. A report of 130 cases. *Panminerva Med*. 23:243–248.
19. Udupa, K.B., and K.R. Reissmann. 1974. Acceleration of granulopoietic recovery by androgenic steroids in mice made neutropenic by cytotoxic drugs. *Cancer Res*. 34:2517–2520.
20. DiBenedetto, J. Jr., D.J. Higby, S.J. Chester, and M.M. Albala. 1980. Reversal of cyclophosphamide induced neutropenia by hypertransfusion and androgen therapy. *J. Med*. 11:385–392.
21. Horn, Y., and D.C. Price. 1972. The effect of androgens on erythroid and granulocytic marrow recovery in the irradiated rat. *Acta Haematol*. 48:300–306.
22. Horn, Y. 1971. The effect of androgenic hormones on bone marrow of rats receiving chemotherapy. *Oncology*. 25:512–519.
23. Horn, Y. 1972. A comparison of two androgenic hormones as leukopoietic agents in irradiated rats. *Oncology*. 26:16–24.
24. Horn, Y. 1971. Leucopoietic properties of four different androgenic hormones in irradiated rats. *Scand. J. Haematol*. 8:470–475.
25. D'Alessandro, N., N. Gebbia, F. Biondo, L. Campio, G. Leto, F. Tumminello, and L. Rausa. 1979. Haemopoietic effects of 7 alpha, 17 beta dimethyltestosterone. *Pharmacol. Res. Commun*. 11:81–94.
26. Sanchez-Medal, L., J. Pizzuto, E. Torre-Lopez, and R. Derbez. 1964. Effect of Oxymetholone in Refractory Anemia. *Arch. Intern. Med*. 113:721–729.
27. Sanchez-Medal, L. 1971. The hemopoietic action of androstanes. *Prog. Hematol*. 7:111–136.
28. Alter, B.P. 1992. Fanconi's anemia. Current concepts. *Am. J. Pediatr. Hematol. Oncol*. 14:170–176.
29. Freedman, M.H., and J.J. Doyle. 1999. Chapter 1: Inherited Bone Marrow Failure Syndromes. *In* Pediatric Hematology. Second edition. J. Lilleyman, I. Hann, and V. Blanchette, editors. p. 23–49.
30. Kennedy, B.J. 1965. Stimulation of hematopoiesis by androgenic hormones. *Geriatrics*. 20:808–815.
31. Rawbone, R.G., and K.D. Bagshawe. 1972. Anabolic steroids and bone marrow toxicity during therapy with methotrexate. *Br. J. Cancer*. 26:395–401.
32. Ibanez, L., A.M. Jaramillo, A. Ferrer, and F. de Zegher. 2005. High neutrophil count in girls and women with hyperinsulinaemic hyperandrogenism: normalization with metformin and flutamide overcomes the aggravation by oral contraception. *Hum. Reprod*. 20:2457–2462.
33. Gaspar, M.L., T. Meo, P. Bourgarel, J.L. Guenet, and M. Tosi. 1991. A single base deletion in the Tfm androgen receptor gene creates a short-lived messenger RNA that directs internal translation initiation. *Proc. Natl. Acad. Sci. USA*. 88:8606–8610.
34. de Koning, J.P., A.A. Soede-Bobok, A.C. Ward, A.M. Schelen, C. Antonissen, D. van Leeuwen, B. Lowenberg, and I.P. Touw. 2000. STAT3-mediated differentiation and survival and of myeloid cells in response to granulocyte colony-stimulating factor: role for the cyclin-dependent kinase inhibitor p27(Kip1). *Oncogene*. 19:3290–3298.
35. Shimozaki, K., K. Nakajima, T. Hirano, and S. Nagata. 1997. Involvement of STAT3 in the granulocyte colony-stimulating factor-induced differentiation of myeloid cells. *J. Biol. Chem*. 272:25184–25189.
36. Furutani, T., T. Watanabe, K. Tanimoto, T. Hashimoto, H. Koutoku, M. Kudoh, Y. Shimizu, S. Kato, and H. Shikama. 2002. Stabilization of androgen receptor protein is induced by agonist, not by antagonists. *Biochem. Biophys. Res. Commun*. 294:779–784.
37. Zhou, Z.X., M.V. Lane, J.A. Kemppainen, F.S. French, and E.M. Wilson. 1995. Specificity of ligand-dependent androgen receptor stabilization: receptor domain interactions influence ligand dissociation and receptor stability. *Mol. Endocrinol*. 9:208–218.
38. Antonio, J., J.D. Wilson, and F.W. George. 1999. Effects of castration and androgen treatment on androgen-receptor levels in rat skeletal muscles. *J. Appl. Physiol*. 87:2016–2019.
39. Chung, C.D., J. Liao, B. Liu, X. Rao, P. Jay, P. Berta, and K. Shuai. 1997. Specific inhibition of Stat3 signal transduction by PIAS3. *Science*. 278:1803–1805.

40. Minami, M., M. Inoue, S. Wei, K. Takeda, M. Matsumoto, T. Kishimoto, and S. Akira. 1996. STAT3 activation is a critical step in gp130-mediated terminal differentiation and growth arrest of a myeloid cell line. *Proc. Natl. Acad. Sci. USA*. 93:3963–3966.
41. Ward, A.C., L. Smith, J.P. de Koning, Y. van Aesch, and I.P. Touw. 1999. Multiple signals mediate proliferation, differentiation, and survival from the granulocyte colony-stimulating factor receptor in myeloid 32D cells. *J. Biol. Chem*. 274:14956–14962.
42. Wang, L., M.O. Arcasoy, S.S. Watowich, and B.G. Forget. 2005. Cytokine signals through STAT3 promote expression of granulocyte secondary granule proteins in 32D cells. *Exp. Hematol*. 33:308–317.
43. Numata, A., K. Shimoda, K. Kamezaki, T. Haro, H. Kakumitsu, K. Shide, K. Kato, T. Miyamoto, Y. Yamashita, Y. Oshima, et al. 2005. Signal transducers and activators of transcription 3 augments the transcriptional activity of CCAAT/enhancer-binding protein alpha in granulocyte colony-stimulating factor signaling pathway. *J. Biol. Chem*. 280:12621–12629.
44. Corey, S.J., A.L. Burkhardt, J.B. Bolen, R.L. Geahlen, L.S. Tkatch, and D.J. Tweardy. 1994. Granulocyte colony-stimulating factor receptor signaling involves the formation of a three-component complex with Lyn and Syk protein-tyrosine kinases. *Proc. Natl. Acad. Sci. USA*. 91:4683–4687.
45. Matsuda, T., and T. Hirano. 1994. Association of p72 tyrosine kinase with Stat factors and its activation by interleukin-3, interleukin-6, and granulocyte colony-stimulating factor. *Blood*. 83:3457–3461.
46. Del Rio, L., S. Bennouna, J. Salinas, and E.Y. Denkers. 2001. CXCR2 deficiency confers impaired neutrophil recruitment and increased susceptibility during Toxoplasma gondii infection. *J. Immunol*. 167:6503–6509.
47. Boulay, F., M. Tardif, L. Brouchon, and P. Vignais. 1990. The human N-formylpeptide receptor. Characterization of two cDNA isolates and evidence for a new subfamily of G-protein-coupled receptors. *Biochemistry*. 29:11123–11133.
48. Bozic, C.R., N.P. Gerard, C. von Uexkull-Guldenband, L.F. Kolakowski Jr., M.J. Conklyn, R. Breslow, H.J. Showell, and C. Gerard. 1994. The murine interleukin 8 type B receptor homologue and its ligands. Expression and biological characterization. *J. Biol. Chem*. 269:29355–29358.
49. Lee, J., G. Cacalano, T. Camerato, K. Toy, M.W. Moore, and W.I. Wood. 1995. Chemokine binding and activities mediated by the mouse IL-8 receptor. *J. Immunol*. 155:2158–2164.
50. Gao, J.L., E.J. Lee, and P.M. Murphy. 1999. Impaired antibacterial host defense in mice lacking the N-formylpeptide receptor. *J. Exp. Med*. 189:657–662.
51. Panopoulos, A.D., L. Zhang, J.W. Snow, D.M. Jones, A.M. Smith, K.C. El Kasmi, F. Liu, M.A. Goldsmith, D.C. Link, P.J. Murray, and S.S. Watowich. 2006. STAT3 governs distinct pathways in emergency granulopoiesis and mature neutrophils. *Blood*. 108:3682–3690.
52. Shim, G.J., L. Wang, S. Andersson, N. Nagy, L.L. Kis, Q. Zhang, S. Makela, M. Warner, and J.A. Gustafsson. 2003. Disruption of the estrogen receptor beta gene in mice causes myeloproliferative disease resembling chronic myeloid leukemia with lymphoid blast crisis. *Proc. Natl. Acad. Sci. USA*. 100:6694–6699.
53. McLemore, M.L., S. Grewal, F. Liu, A. Archambault, J. Poursine-Laurent, J. Haug, and D.C. Link. 2001. STAT-3 activation is required for normal G-CSF-dependent proliferation and granulocytic differentiation. *Immunity*. 14:193–204.
54. Panopoulos, A.D., D. Bartos, L. Zhang, and S.S. Watowich. 2002. Control of myeloid-specific integrin alpha Mbeta 2 (CD11b/CD18) expression by cytokines is regulated by Stat3-dependent activation of PU.1. *J. Biol. Chem*. 277:19001–19007.
55. Hermans, M.H., C. Antonissen, A.C. Ward, A.E. Mayen, R.E. Ploemacher, and I.P. Touw. 1999. Sustained receptor activation and hyperproliferation in response to granulocyte colony-stimulating factor (G-CSF) in mice with a severe congenital neutropenia/acute myeloid leukemia-derived mutation in the G-CSF receptor gene. *J. Exp. Med*. 189:683–692.
56. Redell, M.S., A. Tsimelzon, S.G. Hilsenbeck, and D.J. Tweardy. 2007. Conditional overexpression of Stat3alpha in differentiating myeloid cells results in neutrophil expansion and induces a distinct, antiapoptotic and pro-oncogenic gene expression pattern. *J. Leukoc. Biol*. 82:975–985.
57. Croker, B.A., D. Metcalf, L. Robb, W. Wei, S. Mifsud, L. DiRago, L.A. Cluse, K.D. Sutherland, L. Hartley, E. Williams, et al. 2004. SOCS3 is a critical physiological negative regulator of G-CSF signaling and emergency granulopoiesis. *Immunity*. 20:153–165.
58. Kimura, A., I. Kinjyo, Y. Matsumura, H. Mori, R. Mashima, M. Harada, K.R. Chien, H. Yasukawa, and A. Yoshimura. 2004. SOCS3 is a physiological negative regulator for granulopoiesis and granulocyte colony-stimulating factor receptor signaling. *J. Biol. Chem*. 279:6905–6910.
59. Jenkins, B.J., A.W. Roberts, M. Najdovska, D. Grail, and M. Ernst. 2005. The threshold of gp130-dependent STAT3 signaling is critical for normal regulation of hematopoiesis. *Blood*. 105:3512–3520.
60. Takeda, K., B.E. Clausen, T. Kaisho, T. Tsujimura, N. Terada, I. Forster, and S. Akira. 1999. Enhanced Th1 activity and development of chronic enterocolitis in mice devoid of Stat3 in macrophages and neutrophils. *Immunity*. 10:39–49.
61. Lee, C.K., R. Raz, R. Gimeno, R. Gertner, B. Wistinghausen, K. Takeshita, R.A. DePinho, and D.E. Levy. 2002. STAT3 is a negative regulator of granulopoiesis but is not required for G-CSF-dependent differentiation. *Immunity*. 17:63–72.
62. Welte, T., S.S. Zhang, T. Wang, Z. Zhang, D.G. Hesslein, Z. Yin, A. Kano, Y. Iwamoto, E. Li, J.E. Craft, et al. 2003. STAT3 deletion during hematopoiesis causes Crohn's disease-like pathogenesis and lethality: a critical role of STAT3 in innate immunity. *Proc. Natl. Acad. Sci. USA*. 100:1879–1884.
63. Kamezaki, K., K. Shimoda, A. Numata, T. Haro, H. Kakumitsu, M. Yoshie, M. Yamamoto, K. Takeda, T. Matsuda, S. Akira, et al. 2005. Roles of Stat3 and ERK in G-CSF signaling. *Stem Cells*. 23:252–263.
64. de Koning, J.P., A.A. Soede-Bobok, A.M. Schelen, L. Smith, D. van Leeuwen, V. Santini, B.M. Burgering, J.L. Bos, B. Lowenberg, and I.P. Touw. 1998. Proliferation signaling and activation of Shc, p21Ras, and Myc via tyrosine 764 of human granulocyte colony-stimulating factor receptor. *Blood*. 91:1924–1933.
65. Liu, F., H.Y. Wu, R. Wesselschmidt, T. Kornaga, and D.C. Link. 1996. Impaired production and increased apoptosis of neutrophils in granulocyte colony-stimulating factor receptor-deficient mice. *Immunity*. 5:491–501.
66. Hibbs, M.L., C. Quilici, N. Kountouri, J.F. Seymour, J.E. Armes, A.W. Burgess, and A.R. Dunn. 2007. Mice lacking three myeloid colony-stimulating factors (G-CSF, GM-CSF, and M-CSF) still produce macrophages and granulocytes and mount an inflammatory response in a sterile model of peritonitis. *J. Immunol*. 178:6435–6443.
67. Fried, W., and C. Morley. 1985. Effects of androgenic steroids on erythropoiesis. *Steroids*. 46:799–826.
68. Gardner, F.H., and E.C. Besa. 1983. Physiologic mechanisms and the hematopoietic effects of the androstanes and their derivatives. *Curr. Top. Hematol*. 4:123–195.
69. Beckman, B., B. Maddux, A. Segaloff, and J.W. Fisher. 1981. Effects of testosterone and 5 beta-androstanes on in vitro erythroid colony formation in mouse bone marrow. *Proc. Soc. Exp. Biol. Med*. 167:51–54.
70. Besa, E.C., and L.P. Bullock. 1981. The role of the androgen receptor in erythropoiesis. *Endocrinology*. 109:1983–1989.
71. Mooradian, A.D., J.E. Morley, and S.G. Korenman. 1987. Biological actions of androgens. *Endocr. Rev*. 8:1–28.
72. Claustres, M., and C. Sultan. 1988. Androgen and erythropoiesis: evidence for an androgen receptor in erythroblasts from human bone marrow cultures. *Horm. Res*. 29:17–22.
73. Besa, E.C. 1994. Hematologic effects of androgens revisited: an alternative therapy in various hematologic conditions. *Semin. Hematol*. 31:134–145.
74. Basu, S., G. Hodgson, M. Katz, and A.R. Dunn. 2002. Evaluation of role of G-CSF in the production, survival, and release of neutrophils from bone marrow into circulation. *Blood*. 100:854–861.
75. Dewald, B., and M. Baggiolini. 1986. Methods for assessing exocytosis by neutrophil leukocytes. *Methods Enzymol*. 132:267–277.